Volume 6 OCTOBER, 1935 Number 10

PHYSICS

A Journal of General and Applied Physics

A Study of Arc Temperatures by an Optical Method

C. G. SUITS, *Research Laboratory, General Electric Company*

(Received June 28, 1935)

Sound waves passing through arcs in air are photographed with a rotating mirror camera, whereby the sound velocity in the arc core is determined. From the observed sound velocity the arc temperature may be calculated by a method previously described. The arcs measured by this method, together with the sound velocities and corresponding temperatures, are:

Cored carbon	1.85×10^5 cm sec.$^{-1}$	5500°K
NaCl cored C	1.57	4740
Al cored C	2.14	6160
W cored C	2.17	6220
W 6 mm electrodes	2.04	5950
W 9.5 mm electrodes	2.27	6440
W-Fe	2.13	6150
Fe-Fe welding arc	2.08	6020

The experimental error corresponds to ±100° at 5500°K. The experimental requirements of the sound source are discussed in detail. The gas temperature across the arc core is found to be constant within the error of observation. For most of the arcs studied the current density and electric gradients have also been measured, so that the data may be used as a test of the thermal ionization theory. The "effective ionization potential (I.P.)" of the arc gas is in all cases above the I.P. of the metallic vapor and below that of nitrogen. For the W arcs the effective I.P. is 15 volts, midway between the first I.P. of O_2 and N_2. For the arcs other than tungsten, this quantity is lowered appreciably by electrode vapor. A small partial pressure of Na lowers the arc temperature by approximately 1500°. The temperature of a welding arc between a coated iron welding rod and a steel plate is measured to be 6000°, from which the dissociation of the arc atmosphere is found to be 81 percent. This high degree of dissociation points to the importance of the dissociation-diffusion-recombination process for heat transfer in welding arcs and explains the recently reported negative results of attempts to arc weld in pure argon.

1. INTRODUCTION

AN optical method of observing the passage of sound waves through arcs has been developed and is herewith described. The basis of the method is the experimental fact that a sound "wave" moving through a radiating gas is visible by virtue of the increased luminosity in the high pressure region. This wave front, which travels at a velocity 5 to 8 times greater than the velocity of sound at room temperatures, is photographed by means of a high speed camera; from these photographs the sound velocity is measured and the gas temperature calculated.

This means of determining the sound velocities is superior in simplicity and accuracy to the method previously described,[1,2] and is limited only in that very high luminosity is required in the arc.

2. EXPERIMENTAL METHOD

This experimental method is illustrated in Fig. 1, where the sound produced by a condensed spark discharge in air is passed through an arc and viewed by a rotating mirror camera.

As a sound source, a spark discharge in air is very satisfactory for this purpose. From an extensive literature[3] it is known that an oscillatory or nonoscillatory spark in air produces a single expanding pressure pulse which, for photographic

[1] C. G. Suits, Proc. Nat. Acad. Sci. **21**, 48 (1935); Physics **6**, 190 (1935).

[2] H. Poritsky and C. G. Suits, Physics **6**, 196 (1935).

[3] Mach and Gruss, Wiener. Ber. **78**, 14 (1878); **98**, 277 (1888); Mach and Salcher, Wied. Ann. **32**, 277 (1888); Raps, Wied. Ann. **50**, 193 (1893); Toepler, Ann. d. Physik **14**, 838 (1904); Foley and Souder, Phys. Rev. **35**, 373 (1912); Foley, Phys. Rev. **16**, 449 (1920); J. E. Smith, Phys. Rev. **25**, 870 (1925); Okubo and Matuyama, Phys. Rev. **34**, 1474 (1929).

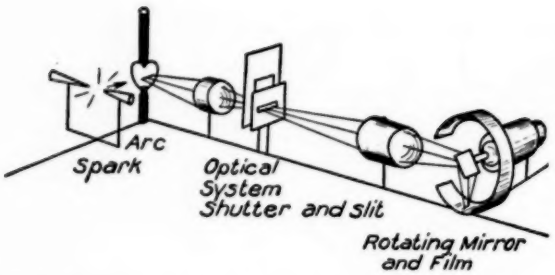

FIG. 1. Apparatus for photographing sound waves in arcs.

purposes, is approximately one mm thick. The velocity of propagation of the "wave" front is initially high but soon attenuates to a constant value of approximately 346 m sec.$^{-1}$ (at 25°C) within a short distance from the source. The distance required for this reduction to normal velocity depends upon the discharge rate, condenser energy, spark voltage, and probably other variables. This point is discussed in more detail below.

By reference to the diagram of Fig. 1, it may be seen that the sound spark is so placed that the electrode axis is parallel to the optical axis of the viewing system. It is apparently necessary to make the observations along an element of the "sound cylinder" since we have failed to obtain readable photographs for any other orientation. The direction of passage of sound through the arc is, however, immaterial. The image of the sound wave in the arc is formed on the slit by a lens. A second lens forms an image of the slit on the cylindrical film which is scanned by the rotating mirror running at high speed. The film holder is so arranged that 10 exposures may be taken on each film. Both lenses have an effective aperture of approximately F3. A spring operated shutter is placed at the slit and is so dimensioned that the time of opening of the slit is one revolution of the mirror, which is approximately 1/300 sec.

The synchronization of the shutter with the sound spark is accomplished with contacts on the shutter which operate the primary of an ignition coil, the secondary of which is connected to a three-sphere gap that triggers the sound circuit. The mirror is rotated on the shaft of a single-phase 180-cycle motor operated at 300 cycles. This motor runs within a percent of synchronism to provide a speed of 18,000 r.p.m. This speed is sufficient to give the required time resolution and cannot be greatly exceeded in the present optical system without photographically underexposing the most intense arcs. The exposure calculated from the slit width, dimensions, and mirror speed is approximately 1/2,000,000 sec., which is insufficient to record some arcs properly, as, for example, the low current copper arc and the low current carbon arc.

The experimental method described is similar to that used by Anderson and Smith[4] and others in studying exploded wires, Beams[5] and others in studying spark discharges, and is similar in principle to the apparatus used by Schonland[6] in the study of lightning discharges.

In the shadow method of sound wave photography first reported by Foley,[3] an image of the sound wave is formed as a "shadow" cast by the high pressure region on the plate. In the present experiment the gas through which the wave passes is luminous and the wave front is observed by virtue of the higher concentrations of radiating particles in the high pressure region. This effect was first found in exploded wire photographs by Anderson and Smith.

3. RESULTS

Three photographic enlargements (approximately ten diameters), from rotating mirror camera films showing sound "waves" in arcs, appear in Fig. 2. Figs. 2a and b were taken for the cored carbon projection arc (case 2 below), Fig. 2c for the iron welding arc (case 8 below). At point 1 of Fig. 2a the exposure of the arc appears; at 2 the sound gap has started to discharge; at 3 the sound front enters the arc and passes through the core, leaving the slanting line, the slope of which is proportional to the velocity of sound. The striations between 2 and 3 are a result of the intense light from the oscillatory sound gap, scattered in the optical system. The portion of this light scattered by the hot arc gas is negligibly small. The wedge shaped structure to the sound "wave" at 3 is a result of the direction of viewing which, it will be remembered, is parallel to the axis of the

[4] Anderson and Smith, Astrophys. J. **64**, 359 (1926).
[5] Beams, Phys. Rev. **35**, 24 (1930).
[6] Schonland and Collins, Nature **132**, 407 (1933).

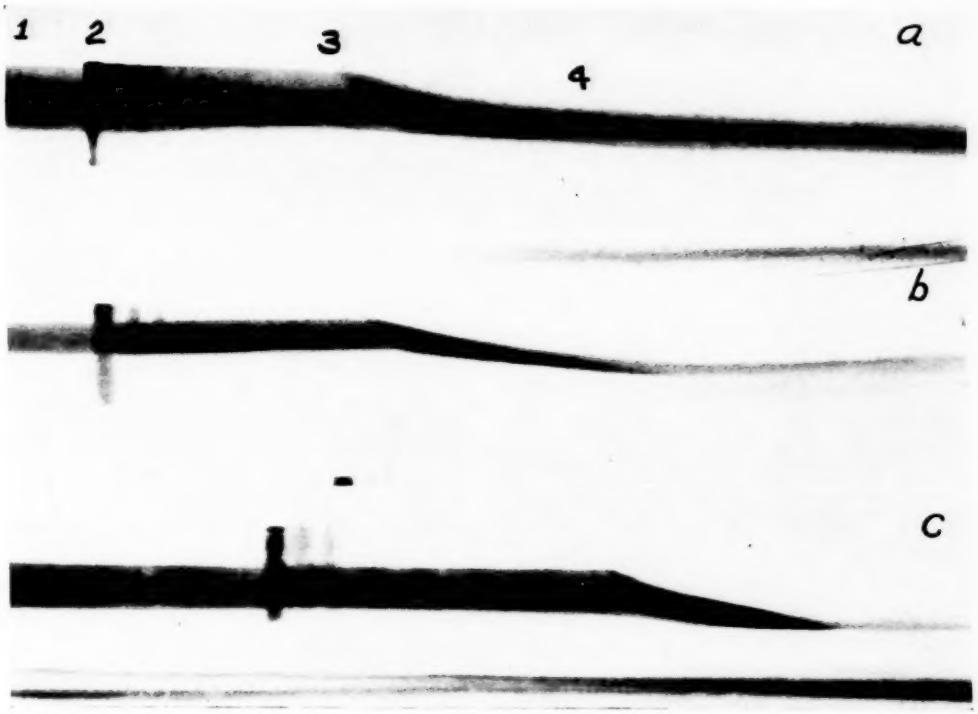

FIG. 2.

sound gap but perpendicular to the axis of the arc. We have taken some photographs from a direction parallel to both the spark and arc axes, and in this case the wave front appears as a line rather than a wedge. In the best records, of which the above are examples, the definition is such that the uncertainty in reading the slope of the wave front is about three percent, which at 5500°K corresponds to an uncertainty of $\pm 60°$ in the temperature.

This is probably the largest single source of error in the method. Other errors, in calibration, motor speed, and the like, increase the error to a total of about five percent or $\pm 100°$ temperature uncertainty. The spread of the measurements is in most cases greater than this, especially with the high current welding arcs, which at best are erratic and quasi-stable. This spread must therefore be interpreted as a real temperature fluctuation; it would be remarkable if the welding arc temperature did not fluctuate since the current density and other quantities vary. An indeterminate amount of error is involved in the extrapolation of the equilibrium constants of the air dissociation for the temperatures above 5000°K. The uncertainty in this extrapolation cannot be very large, however, since the asymptotic limits to the composition of the air are known.

This method of measuring arc temperatures is simple and rapid. A film with ten traces may be taken very quickly, and on the average there are about three satisfactory records per film, each a rather accurate determination of temperature and temperature gradients, if any.

4. SOUND REQUIREMENTS

We have obtained satisfactory photographs of wave fronts in arcs for values of capacitance between 0.15 and 1.2 mf at 33 kv, providing the discharge rate is sufficiently high. Flat-rolled tinfoil paper condensers are generally unsatisfactory because of the high inductance and resistance. In particular, for 1.2 mf and 33 kv, a discharge frequency of 100 kc is satisfactory, whereas the same capacitance and voltage at 30 kc have not produced readable wave fronts.

Near a source of intense sound the velocity may be very much greater than the normal value of 0.346×10^5 cm sec.$^{-1}$ (25°C), and the question

TABLE I.

1 Capacitance (mf)	2 Sound velocity at 5 cm (25°C) (cm sec.$^{-1}$)	3 Sound velocity at 10 cm (25°C) (cm sec.$^{-1}$)	4 Sound velocity* in projection carbon arc, 5 cm from source (cm sec.$^{-1}$)
1.2	$.585\times10^5$	$.525\times10^5$	1.81×10^5
.6	.440	.390	1.84
.3	.402	.365	1.83
.15	.380	.350	—

* Averages of 10 experimental values.

arises as to the possible effect of this abnormal velocity on the measured velocities in the arc. It may be shown[2] that the temperature gradients between the arc core and the surrounding air would be expected to lead to increased convexity of the wave front and decreased energy density, and, as a result, a rapid reduction of abnormal velocities. This prediction has now been verified in experiments in which sound waves of normal and abnormal velocities have been passed through a highly reproducible and stable arc where the velocities are measured at the arc temperatures.

The results are tabulated in Table I where the first column gives the capacitance used at a potential of 33 kv in the sound circuit. In columns 2 and 3 are shown the sound velocities in air at 25°C at distances of five cm and ten cm, respectively, from the sound source, measured by a cathode-ray oscillograph method.[1] In the fourth column is the sound velocity of the cases listed in column 2 as measured in a carbon arc under constant conditions. It may be seen that the velocity measured in the arc is constant to within two percent for sound waves which in air at room temperatures have velocities ranging between 15 and 70 percent above normal. We conclude from this fact that no appreciable error arises from the abnormal velocity effect in the observed range.

The velocity of sound method as described has been used to measure the temperatures of a number of arcs in air at atmospheric pressure; a condensed list of these results is given in Table II. In all of the cases observed the temperatures lie in the range 4000°–7000°K. Because of the variety of experimental conditions, the arcs listed in the above table will be described in detail separately.

TABLE II.

Arc	1 Temp. °K	2 Electron density $n\times10^{-14}$	3 Effective I.P. of arc gas V_{ie}	4 I.P. of chief metallic element V_m
(A) Copper	4050	.39*	9.5*	7.69
(B) Cored projection C	5500	1.59	11.7	6.9
(C) NaCl cored C	4740	7.2	8.7	5.11
(D) Al cored C	6160	1.09	13.6	5.95
(E) W cored C	6220	.24	15.3	8.1
(F) 6 mm W	5950	.25	14.7	8.1
(G) 9.5 mm W	6440			
(H) W welding arc	6150			
(I) Coated Fe welding arc	6020			

* Included here as a correction to values previously published in 2.

Where possible, the current density I and electric gradient E in the arc column also have been measured for the experimental conditions used in the temperature determinations. These values are also given below.

It would be desirable to compare the measurements of arc temperature by the velocity of sound method with similar determinations by other methods. The copper arc temperatures (case (A)) were taken for experimental conditions nearly identical with those used by von Engel and Steenbeck[7] and may be compared with their value of $4600°\pm350°$. The hope of taking measurements by the present method of identical cases studied by Ornstein[8] and his coworkers by the band spectra method has been fulfilled in only one case since most of the arcs of sufficient luminosity for sound wave photographs have the bands masked by continuous spectrum. However, in the case of the Al cored carbon arc, the experimental conditions which we have used are sufficiently near those reported by Ornstein and Brinkman[8a] to make the results comparable. The temperature in the violet core of this arc found by the band spectrum method is $6000°K\pm300°K$ for an arc length of 1.5 cm and a current of 7 amperes. The value which we have found for substantially the same case is 6160°K with a spread of $\pm200°K$. From these two cases it appears that the results obtained

[7] von Engel and Steenbeck, Wiss. Veroff. a. d. Siemens-Konzern **10**, 155 (1931); **12**, 74 (1933); **12**, 89 (1933).

[8] See Ornstein, *His Life and Work*, for references given therein.

[8a] Ornstein and Brinkman, Proc. Amst. Akad. Sci. **34**, 498 (1931).

by the velocity of sound method are in good agreement with temperature measurements obtained by two entirely different methods.

(A) Copper arc 4050°K

The measurements were made on the arc between water-cooled copper electrodes in a stabilizing air stream tube. The results[1] are: For arc lengths between 3 and 12 cm at a current of 6 amperes, and for a constant arc length of 9 cm and currents varying between 3 and 26 amperes, the sound velocity is found to be 1.38×10^5 cm sec.$^{-1}$. The (positive column) current density is 10 ± 2 amperes cm^{-2} throughout the current range, while the electric gradient in the arc column is 16.5 volts cm^{-1} at 6 amperes.

(B) Cored carbon arc 5500°K

This arc uses a cored carbon cathode[9] and anode[10] burning freely in air, anode above, at an arc length of 1.1 cm (average), and a current of 45 amperes. The current density is 50 amperes cm^{-2} and the gradient 10 volts cm^{-1}. 36-mm motion picture projectors commonly use this arc as a light source. The sound velocity and temperature, measured midway between the electrodes (as in all cases described below), are respectively 1.85×10^5 cm sec.$^{-1}$ and *5500*°K.

(C) NaCl cored carbon 4740°K

In this arc a cored carbon cathode[10] was used as the top electrode, while the lower electrode, the anode, was drilled and filled with NaCl. The portion of the arc column near the cathode is white and distinct from that portion near the anode, which has the characteristic Na yellow. The observations were made in the Na column. At an arc length of 5.6 cm, and a current of 43 amperes, for which the current density is 85 amperes cm^{-2} and the gradient 6 volts cm^{-1}, we find a sound velocity of 1.57×10^5 cm sec.$^{-1}$, corresponding to the temperature of *4740*°K.

(D) Al cored carbon 6160°K

The lower electrode was 8 mm carbon, drilled and filled with Al powder; the upper electrode, the cathode, was an 8 mm cored carbon.[9] At 43 amperes and 4.2 cm arc length, for which the current density is 38 amperes cm^{-2} and the gradient 7.9 volts cm^{-1}, we observe a sound velocity of 2.14×10^5 cm sec.$^{-1}$, corresponding to an arc temperature of *6160*°K.

(E) W cored carbon 6220°K

In this arc the lower electrode, the anode, was an 8 mm carbon drilled and filled with tungsten powder. The cathode was cored carbon.[9] At 40 amperes and 4.2 cm arc length, with a current density of 18 amperes cm^{-2} and gradient of 17 volts cm^{-1}, we find a sound velocity of 2.17×10^5 sec.$^{-1}$ and an arc temperature of *6220*°K.

(F) Tungsten 5950°K

Solid tungsten rods of 6 mm diameter burning vertically in air (anode above) were used in this experiment. With this diameter of electrode it is found that 5.5 amperes is the maximum current which can be used without developing instability in the arc. At 1.6 cm arc length the current density is 20 amperes cm^{-2} and the gradient 22 volts cm^{-1}. We find a sound velocity of 2.04×10^5 cm sec.$^{-1}$, corresponding to a temperature of *5950*°K.

(G) Tungsten 6440°K

With 9.5 mm solid tungsten rods as electrodes (cathode above), it is possible to use a current of 25 amperes with sufficient stability to allow rotating mirror photographs to be made. This arc is, however, relatively unsteady and but few of the exposures were readable. A large spread in the measurements, much greater than the experimental error, indicates an actual temperature fluctuation which is characteristic of the instability. Fluctuations in light intensity and arc voltage[11] probably correlate with these temperature variations. The average sound velocity is 2.27×10^5 cm sec.$^{-1}$, nearly 7 times the value at 0°C. The temperature corresponding to the average velocity is *6440*°K; the limits of temperature fluctuation are *5900*°K and *7600*°K (estimated), the latter being the highest observed in this experiment.

[9] National Carbon Co., 5/16″ Orotip cored.
[10] National Carbon Co., High-Low Projector.
[11] C. G. Suits, Physics **5**, 380 (1934).

5. Temperatures of Welding Arcs

These arcs were used under conditions as nearly as possible like those employed in practical welding operations. The current was supplied by a conventional welding generator, and the arc length and current were adjusted under the direction of a welder to values appropriate for the electrodes, polarity, and work. These arcs, like all welding arcs, are relatively unstable. The arc voltage, light intensity, position, current density, and probably other quantities vary in an irregular manner. It was necessary to take a great many records to obtain suitable data, but some excellent exposures were secured for both cases (see Fig. 2c). The arc temperature partakes in the fluctuation, so that the spread of the measurements was great.

(H) Tungsten-iron 6150°K

For heating, but not depositing metal, the welder uses a 3.2 mm solid tungsten rod as cathode. At an arc length of 0.5 cm and a current of 80 amperes, the current density varies between 80 and 110 amperes cm^{-2}. The average sound velocity is found to be 2.13×10^5 cm $sec.^{-1}$ and the average temperature *6150*°K. The temperature fluctuates between the limits *5000*°K and *7000*°K (estimated).

(I) Iron-iron 6020°K

In this measurement a 3/16″ type W-20 coated welding rod was used as cathode above a large steel plate. The current was 125 amperes at an arc length of 1 cm. The current density fluctuates between 94 and 405 amperes cm^{-2}. The observed average sound velocity is 2.08×10^5 cm $sec.^{-1}$, corresponding to an arc temperature of *6020*°K. The temperature fluctuation lies between the limits *4400*°K and *7000*°K (estimated).

6. Discussion of Results

For all of the cases here reported the sound velocities across the core are sensibly constant, as shown by the constant slope on the photographic records, which means that the temperature across the core of the arc must be constant within approximately 120°, which is the uncertainty in reading the slope on the film.

The cores of the atmospheric pressure arcs studied are therefore regions of substantially constant high gas temperatures. The gradient between the core temperature and room temperature must occur in the photographically nonluminous boundary layers of the arc column.

The data of Table I allow a test of the thermal ionization theory of high pressure arcs first proposed by Compton.[12] For that purpose the electron density n has been calculated from

$$n = I/eKE,$$

where I is the observed current density, e is the electronic charge, E is the electric gradient in the arc column, and K is the mobility. The mobility K is calculated from Wahlin's[13] experimental values of the electron mobility, assumed to vary as $(T)^{\frac{1}{2}}$ and corrected for the effect of dissociation on the mean free path. This latter correction is numerically three times at a temperature of 6000°K. The correction for field is negligibly small.

For this electron density n, the effective ionization potential V_{ie} is calculated as follows: Using the Saha equation[14] it is assumed that n is produced by a homogeneous gas of ionization potential V_{ie} at the measured temperature and at a pressure of one atmosphere.

This effective ionization potential V_{ie} (column 3, Table II) may then be compared to the ionization potential of $N_2 = 16.7$ volts, of $N = 14.5$ volts, of $O_2 = 14.1$ volts, of $O = 13.6$ volts, and finally to V_m (column 4, Table II), the ionization potential of the chief metallic element in the arc. It may be seen that V_{ie} is, within the spread in the measurements, less than 16.7 and greater than V_m for all cases tested. For the W arcs $V_{ie} \gtreqless 15$ volts, which is about midway between the ionization potential of O_2 and N_2. From this we may conclude that the metallic vapor from the electrodes does not contribute appreciably to the ionization in the tungsten arc. The agreement between V_{ie} and the ionization potentials of oxygen and nitrogen is about as good as can be expected for the relatively complicated experimental conditions, and provides strong evidence for the essential correctness of theory.

---

[12] K. T. Compton, Phys. Rev. **21**, 266 (1923).
[13] Wahlin, Phys. Rev. **27**, 169 (1924).
[14] Compton and Langmuir, Rev. Mod. Phys. **2**, 123 (1930).

In the cases of the other arcs in Table II the effective ionization potential of the arc gas is decreased by the presence of the low ionization potential metallic vapor from the electrodes. Judging by the comparative values of V_{ie} and V_m, the effect is not simply related to the ionization potential of the metal. In general it is probably necessary to take account also of the electrode volatility and chemical properties.

The observed constancy of the current density in the copper arc is compatible with a variable gradient on two grounds: (a) the electron mobility has a dependence on field strength; and (b) a temperature variation with current may be occurring within the limits of experimental accuracy. It is not possible to decide between these two cases without greater accuracy in the temperature measurements, but it is true that the dependence of mobility on field strength is sufficient to allow a constant current density at constant temperature (and hence n) within the limits of measurement of I.

The interesting effects produced in the arc by the introduction of sodium vapor are: (1) a reduction in arc temperature; (2) an increase in current density; and (3) a decrease in gradient. The removal of metallic vapor by the use of W electrodes produces the reverse effect. This behavior is to be expected on theoretical grounds.

The observation that the W arc in air is an "air" arc raises some questions concerning the causes of its high luminosity. The partial pressure of W vapor is very small, yet the luminosity is greater than any other case studied. It is also true that the electrodes are rapidly consumed in air, and that the spectrum is predominantly continuous. In pure hydrogen, however, W electrodes evaporate very slowly and the discharge is practically colorless.

These facts indicate that the high luminosity is due to incandescent tungsten oxide. It is probably true that these particles are in equilibrium with the hot arc gas, but that is speculation at present.

Welding arcs

The measurements on the welding arc fix the average temperature at 6000° and the limits of temperature fluctuation at 4400° and 7000° for this type of discharge. The type W-20 coated welding rod arc represents about the most stable type of welding arc in common use.

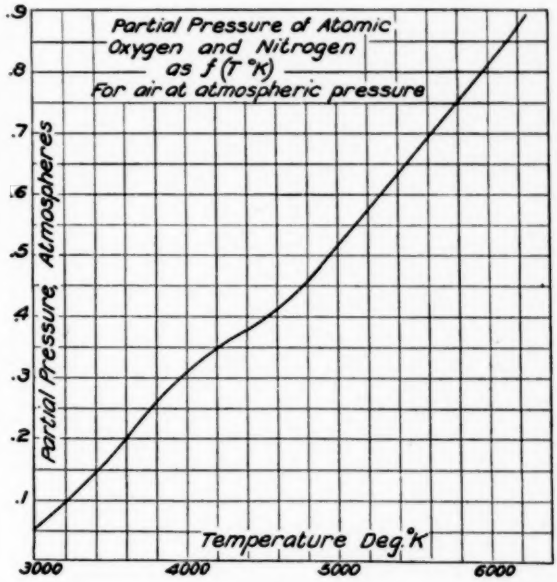

FIG. 3.

As already pointed out, a small amount of metallic vapor of low ionizing potential lowers the arc temperature, increases the current density, and decreases the gradient. The first and third of these factors contribute to arc stability. It is probable that one important function of the coating material of welding rods is to provide this low ionizing potential vapor.

From a knowledge of the welding arc temperature and recently determined[15] equilibrium constants for the dissociation processes

$$O_2 \rightleftharpoons 2\,O$$
$$N_2 \rightleftharpoons 2\,N$$

we may specify the degree of dissociation in welding arcs. In Fig. 3 are shown the total partial pressures of the atomic fractions in dissociated air at atmospheric pressure. At the temperature of the welding arc, 6000°K, 81 percent of the arc atmosphere is atomic oxygen and nitrogen. The effectiveness of dissociated gas in heating metallic surfaces, which act as catalysts for the recombination process, is well known[16] and be-

[15] Giauque and Clayton, J. Am. Chem. Soc. **55**, 4887 (1933); Johnston and Walker, J. Am. Chem. Soc. **55**, 179 (1933); **55**, 191 (1933).

[16] Wood, Proc. Roy. Soc. **A102**, 1 (1922); Phil. Mag. **44**, 538 (1922); Langmuir, Gen. Elec. Rev. **29**, 153 (1926).

lieved to be of importance in atomic hydrogen welding. The high degree of dissociation in welding arcs in air, however, means that these arcs are properly regarded as atomic oxygen-nitrogen arcs which depend to some extent upon the same recombination process for heat transfer. The heat transferred by the diffusion of dissociated gas is proportional to f the fraction of the molecules dissociated, D the diffusion coefficient, and V the dissociation potential. In comparison to hydrogen, nitrogen has a smaller coefficient of diffusion but a larger heat of recombination. The relative magnitude of the heat h_H transferred by the diffusion of H through H_2 and h_N for N through N_2 may be calculated from the ratio:

$$\frac{h_H}{h_N}=\frac{kf_HD_HV_H}{kf_ND_NV_N}=\frac{\lambda_HC_HV_H}{.8\lambda_NC_NV_N},$$

where k is a constant, λ is the mean free path, C is the "molecular velocity," and the subscripts refer to the respective gases. If we assume the temperature to be the same for both cases, using

$$V_H = 4.4 \text{ volts},$$
$$V_N = 11.7 \text{ volts},$$

we find that

$$h_H/h_N = 3.3.$$

Thus, when the relative degrees of dissociation (f_H assumed to be 1), diffusion coefficients, and dissociation potentials are taken into account, the diffusion heat transfer by atomic nitrogen is about one-third as effective as by atomic hydrogen at 6000°K arc temperature. The temperature of the atomic hydrogen arc with 1.5 mm electrode separation, in the current range 4–8.5 amperes, has been measured by Ornstein, Eymers, and Wouda,[17] who find $T=4900°-6300°$K, with a dependence upon current. As shown by Langmuir,[16] the heat transfer by direct conduction is very small compared to that transferred by diffusion, so that we must conclude that the diffusion process is of major importance to the functioning of the welding arc in air.

Experimental evidence supporting these conclusions is found in the negative results of recent attempts[18] to arc-weld in an atmosphere of pure argon. It is found that at the same or greater arc wattages which produce satisfactory welds in air there is a marked lack of pool formation and fusion of the deposited metal, indicating an ineffective heat transfer. The absence of a dissociation process in the monomolecular argon is probably accountable for these results.

[17] Ornstein, Eymers, and Wouda, Proc. Amst. Akad. Sci. **34**, 505 (1931).
[18] Doan and Schulte, Phys. Rev. **47**, 783 (1935).

Shot Effects of Secondary Electron Currents

LUCY J. HAYNER, *Columbia University**

(Received July 12, 1935)

The shot effect of secondary electron currents from plates of triode tubes was measured at 10^5 cycles. Calculations of the electronic charge from shot effects of temperature-limited primary currents, to check the method, agreed with Millikan's value within 1 percent. Measurements were made on five tubes having different secondary emissivities. The average number of secondaries per primary electron, ω, ranged from *1* to *4.5*. The variation of ω with energy of the primaries is shown to agree qualitatively with existing theory. In every case the shot effects of both grid and plate currents were measured. Campbell's general expressions for the shot effect of secondary emission plate currents were extended to grid currents. From the observed differences between grid and plate shot effects it is concluded that secondary emission and primary impact are simultaneous within 10^{-6} second or less. The large shot effects found at high values of ω are correlated with the fluctuations of ω from one impact to another. A qualitative analysis of secondary emission processes shows that, from these data, information can be obtained as to the number of reflected primary electrons and the number of primaries which emit no secondaries. The results obtained are in reasonable agreement with data obtained by other methods.

INTRODUCTION

IN their paper on the shot effect, in 1925, Hull and Williams[1] described a single measurement on the shot effect of secondary electron emission from the plate of a vacuum tube. This measurement was made at 750 kilocycles under experimental conditions such that the average current of secondary electrons was just equal to the average primary current, so that the net plate current was zero. They concluded from their results that emission of secondary electrons was "independent" of the primary impact. The primary current in their tube was partially space-charge limited. The present paper is a report of measurements on a number of tubes under conditions in which the complication due to space charge was not involved, and with secondary currents up to *4.5* times the primary current.

THEORY OF SECONDARY EMISSION SHOT EFFECT

Stimulated by the work of Hull and Williams, and following his own papers on fluctuation phenomena in general, Campbell[2, 3] has derived an expression for the shot effect of a plate current consisting of primary and secondary electrons. He has considered two cases: (1) that in which the emission of secondary electrons is "simultaneous" with the impact of the primary, and (2) the case in which these events are "independent." The exact significance of the terms simultaneous and independent involves the fundamentals of the theory of the shot effect. Fry[4] and others have shown that the properties of the measuring circuit must be considered in any attempt to connect measurements on shot effect with the fluctuations of the electron stream. They begin with the fact that a single electron striking the plate is equivalent to a charge placed on the condenser of the plate circuit. They then assume that this charge is dissipated by an aperiodic or oscillatory current given by the ordinary theory of transient currents. Some experimental support for this assumption lies in the fact that the work functions of metals can, in order of magnitude at least, be calculated from the classical image force. They then compute the desired result, the power dissipated in the circuit, by summing the effects due to the individual electrons.

Campbell considers the effect on the circuit of two separate events, (1) the arrival of a primary electron, and (2) the departure of a secondary. If the transient current produced by the primary is completely neutralized by the opposite current due to the secondary, the two events are "simultaneous." The net effect on the circuit is then zero. If there is no neutralization, the two

* This work was done 1926–28 in the Research Laboratory of the General Electric Company. See L. J. Hayner and A. W. Hull, Phys. Rev. **33**, 281A (1929).

[1] A. W. Hull and N. H. Williams, Phys. Rev. **25**, 147 (1925).

[2] N. R. Campbell, Proc. Camb. Phil. Soc. **15**, 117, 310, 513 (1909–1910).

[3] N. R. Campbell, Phil. Mag. **50**, 81 (1925).

[4] T. C. Fry, J. Frank. Inst. **199**, 203 (1925).

events are "independent." The net effect is then the sum of the separate effects. Evidently the two events will always be registered as simultaneous if the time interval between them is small compared with the period of the circuit, if oscillatory, or to its time constant, if aperiodic. On the other hand, if the interval between the events is long compared to the period or time constant, then in most cases the events will be registered as independent. In one possible but improbable case, if the time interval between the two events is exactly equal to a small multiple of the circuit period, the effect on the circuit will be nearly the same as if the effects were simultaneous.

In case there is more than one secondary electron, an additional time factor enters, namely the time between the emission of the several secondary electrons. In Campbell's derivation, he has tacitly assumed that all the several secondaries come off simultaneously even when they are independent of the primary. The result for the case when the several secondaries come off independently of each other as well as of the primary is also given below.

It is assumed that the arrival of the primary electrons is completely random. There is every reason to believe that temperature limited currents fulfill this condition. If N is the average number arriving at the plate per second, and $\overline{X^2}$ the mean square deviation from N, we have, by the definition of random,

$$\overline{X^2}=N=i_0/e, \tag{1}$$

where i_0 is the average plate current and e the electronic charge.

Let each primary electron produce an average number ω of secondaries. Let the mean square deviation from ω be $\overline{\eta^2}$. The average number of electrons gained by the plate per second will then be $N(1-\omega)$. Let the mean square deviation from this number be $\overline{X_p^2}$. Campbell[3] shows that if the emission of the secondaries is simultaneous with the arrival of the primaries, the result is

$$\overline{X_p^2}=(i_0/e)\{(1-\omega)^2+\overline{\eta^2}\} \quad \text{(simultaneous)}. \tag{2}$$

If the emission of all secondaries is simultaneous, but is independent of the time of impact of the primaries, then

$$\overline{X_p^2}=(i_0/e)\{1+\omega^2+\overline{\eta^2}\} \quad \text{(half independent)}. \tag{3}$$

In addition there is the case not considered by Campbell in which the secondaries are independent of the primary and of each other.

$$\overline{X_p^2}=(i_0/e)\{1+\omega\} \quad \text{(independent)}. \tag{4}$$

$\overline{\eta^2}$ has no meaning in this case, since the secondary current, like the primary, is completely random.

These equations may be applied directly to a system composed of a filament emitting electrons, surrounded by a grid and a plate. The grid is made sufficiently positive to produce saturation of the electron stream. The plate is kept at a positive potential lower than that of the grid, so that secondary electrons emitted by the plate are collected by the grid. Secondary electrons emitted by the grid do not escape from the grid and are not observed.

Let the average number of electrons emitted by the filament per second be $N=i_0/e$. Some fraction ϕ of these will be caught by the grid. This fraction will depend upon the geometry of the tube and the relative values of grid and plate potentials. Then $(1-\phi)N$ per second will strike the plate so that (2), (3), and (4) now become

$$\overline{X_p^2}=(1-\phi)(i_0/e)\{(1-\omega)^2+\overline{\eta^2}\}, \tag{5}$$

$$\overline{X_p^2}=(1-\phi)(i_0/e)\{1+\omega^2+\overline{\eta^2}\}, \tag{6}$$

$$\overline{X_p^2}=(1-\phi)(i_0/e)\{1+\omega\}. \tag{7}$$

The mean square deviation $\overline{X_g^2}$ of the current to the grid is also of interest. The $N\phi$ primary electrons collected by the grid are completely random and independent of the $(1-\phi)N$ primaries giving rise to secondaries at the plate. Hence

$$\overline{X_g^2}=(i_0/e)\{\phi+(1-\phi)(\omega^2+\overline{\eta^2})\} \tag{8}$$

for the simultaneous and half independent cases, and

$$\overline{X_g^2}=(i_0/e)\{\phi+(1-\phi)\omega\} \tag{9}$$

for the fully independent case.

So far, only the fluctuations of the electron stream have been discussed. These fluctuations ultimately cause a deflection of a meter in the output circuit of an amplifier. The value of this deflection, of course, involves the properties of

the shot effect tube and the circuits associated with the tube and amplifier. Several methods have been devised for taking these properties into account, by means of a comparison between the deflection due to the shot effect and the deflection produced by a measured sinusoidal voltage introduced into the system at some point. The theory of any such method, when applied to a pure temperature-limited current, gives J, the average electron current, as a function of e, the circuit constants, and the measured value of the comparison voltage. The comparison between theory and experiment consists in comparing the current thus computed with the current i_0 read on a d.c. meter. If similar methods are applied to currents which are not purely random, or do not involve single electrons, the calculated value of J will represent that random current whose fluctuations would equal the fluctuations actually occurring. The value of J thus computed may be less than i_0, as in space-charge limited currents, or greater, as in the flicker effect.

To connect the computed values of J with the expressions for the fluctuations, it is only necessary to use Eq. (1) in combination with one of the Eqs. (2) to (9). For instance, from (1) and (5), and (1) and (8), using J_p and J_g to distinguish the plate and grid shot effects, respectively,

$$J_p/e=\overline{X_p^2}=(1-\phi)(i_0/e)\{(1-\omega)^2+\overline{\eta^2}\}, \qquad (5a)$$

$$J_g/e=\overline{X_g^2}=(i_0/e)\{\phi+(1-\phi)(\omega^2+\overline{\eta^2})\}, \qquad (8a)$$

and similar equations from (6), (7) and (9).

Certain very important conclusions may be drawn from Eqs. (5a) to (9a) without any knowledge of ω or $\overline{\eta^2}$. If the difference J_g-J_p is formed,

$$J_g-J_p=i_0\{1-2(1-\phi)(1-\omega)\}$$
simultaneous (10)

$$J_g-J_p=i_0\{\phi-(1-\phi)\}$$
half independent or independent. (11)

The values of ϕ found under the conditions of this work range from *0.20* to *0.88*. The right side of (11) may therefore be either positive or negative. The right side of (10) is positive if, as in these experiments, $\omega>1$, and reduces to i_0-2i_p. Here i_p is the average plate current, and is to be taken positive if the plate gains electrons; its value is read from the d.c. plate meter. Hence Eq. (10) may be tested without knowing ω, $\overline{\eta^2}$ or even ϕ. It may be stated here that the results to be described below confirm (10) and exclude (11) as a possibility.

From (8a) and (9a) $\overline{\eta^2}$ may be computed. It should be pointed out that in so doing the correctness of Campbell's theory is assumed in order to derive information about $\overline{\eta^2}$.

$$\overline{\eta_p^2}=J_p/(1-\phi)i_0-(1-\omega)^2 \qquad (12)$$

from measurements on the plate current.

$$\overline{\eta_g^2}=(J_g-\phi i_0)/(1-\phi)i_0-\omega^2 \qquad (13)$$

from measurements on the grid current. The two values of $\overline{\eta^2}$ thus obtained from a given set of data should agree. The determination of ϕ, ω and $\overline{\eta^2}$ will be discussed below.

Experimental Method

At the beginning of the work measurements were made with a resistance coupled amplifier and a shot circuit tuned to 96.6 kc. The method of Hull and Williams was followed; this involves introducing the comparison voltage directly across the first stage of the amplifier, together with a measurement of the equivalent series resistance of the shot circuit. The amplifier, however, had a linear and nearly flat frequency response curve, which eliminated the laborious calculations of the amplification factor F in the Hull and Williams method.

The values of e calculated from temperature limited shot effects observed with this apparatus were always from eight to fifteen percent too low. The amplifier was therefore discarded in favor of the tuned-circuit amplifier described below. Subsequently it was discovered that, due to penetration, a correction of about 5 percent to the calculated inductance of the inductance potentiometer was necessary. This was in such a direction as to bring the e values within $+2$ percent and -5 percent of the correct value. The remaining discrepancies were probably due to insufficient shielding.

A number of shot effect measurements on secondary emission were made with this amplifier

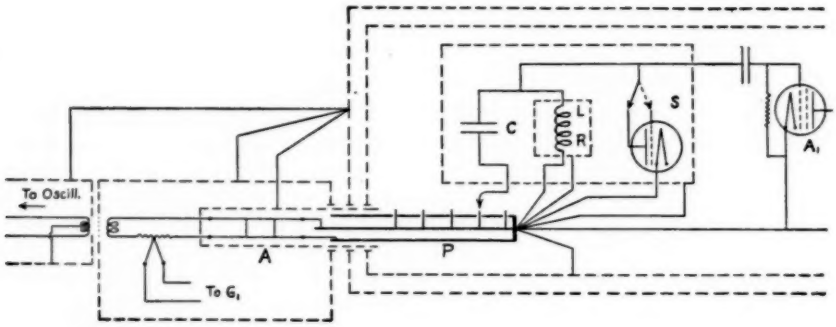

Fig. 1 Circuit diagram of the shot effect apparatus, showing the shielding in broken lines. A_1, first amplifier tube; S, shot tube; P, inductance potentiometer; A, attenuator; G_1, input galvanometer.

by using a comparison method. Measurements of temperature limited shot effect were made frequently during the secondary emission observations, and the e calculated from the former was used in calculating the J's for the latter. In the light of the subsequent discovery of the correction factor, the results obtained in this way are believed to have about the same precision as the later results, and they are therefore included in this report.

Most of the shot effect measurements were made with a tuned shot circuit of natural frequency 99.5 kc and a tuned-circuit-coupled amplifier. The sinusoidal calibration voltage was introduced into the shot circuit according to the method of Williams and Vincent[5] in which an inductance potentiometer of very low impedance is connected permanently in series with the inductance or capacity of the shot circuit. The shot effect equation in this case is

$$i_0=(C^2\omega_0^2/2e)(v_1^2/A), \qquad (14)$$

where i_0 is the average temperature limited electron current; C is the total capacity of the shot circuit; $\omega_0/2\pi$ the resonant frequency of the shot circuit and amplifier; e the electronic charge; v_1 the sinusoidal voltage which, when introduced into the shot circuit, gives the same deflection in the output system of the amplifier as the mean square shot voltage due to i_0; and A is an amplification factor defined below. If the calibration voltage is furnished by a length l of an inductance potentiometer of inductance L_1 per unit length, carrying a current kI_1, where k is an attenuation factor, then

$$i_0=(C^2\omega_0^4k^2lL_1^2/2e)(I_1^2/A). \qquad (15)$$

Here $A=\int_0^\infty\psi(f)df$, where $\psi(f)$ is the amplification at frequency f, $\psi(f_0)$ being set equal to 1. $\psi(f)$ is obtained from the power output of the amplifier when the frequency is varied, keeping the current kI_1 through the inductance potentiometer constant.

The method of Williams and Vincent has several advantages. First, any regeneration present produces the same effect in the amplification of the mean square shot voltage as in that of the calibration voltage. Second, no measurement of resistance is necessary. Another advantage is that the amplification factor A is easily calculated. The method has several disadvantages, all of which are connected with shielding problems. These will be discussed below.

The Apparatus

The amplifier was similar to that described by Hull and Williams. There were five stages, the first four having 222 tubes and the last a 201A. In the last stage high plate voltage and large negative grid bias were used to insure linear amplification of very large signals. The stages were coupled with tuned circuit impedances. Suitable chokes and bypass condensers were inserted in all battery and galvanometer leads to prevent regeneration.

The output detector was a 700-ohm thermocouple inductively coupled to a coil in the plate circuit of the last tube. The thermocouple for measuring the input currents (see Fig. 1) was

[5] N. H. Williams and H. B. Vincent, Phys. Rev. **28**, 1250 (1926).

calibrated with d.c. The deflections of its galvanometer were accurately proportional to the square of the calibrating current. The deflections of the output galvanometer produced by the sinusoidal calibrating voltage were exactly proportional to the deflections of the input galvanometer; showing that the output thermocouple was a square detector. This is essential to the method. The input and output galvanometers were mounted together on a Julius suspension. Both zeros were constant within 0.1 mm.

The shot circuit and the method of applying the calibrating voltage are shown in Fig. 1. The capacity C includes the distributed capacity of the coil, the capacity to ground of the grid or plate of the shot tube, and of the grid of the first amplifier tube, and the capacity of all the connections to ground. Its value was 2318 micro-microfarads, ± 0.1 percent.

The sinusoidal voltage was supplied by a pliodynatron oscillator[6] with a frequency of 99.5 kc. The frequency was measured with a General Radio precision wave meter with an estimated precision of 0.1 percent. This frequency was at all times constant within the limits of the precision of measurement.

The inductance potentiometer was similar to that described by Hull and Williams and others. It was made entirely of brass and very carefully constructed. A correction[7] of about 5 percent for penetration was necessary in calculating L_1. The value of L_1 was 3.746×10^{-9} henry ± 0.1 percent. The same oscillator and inductance potentiometer were used with both amplifiers.

When the calibration voltage is applied in series with the shot circuit as shown in Fig. 1, the voltage required from the inductance potentiometer is very small. In this case it was less than 1/100 of the voltage which would have been required if the calibrating voltage had been applied directly on the grid of the first amplifier tube. In order that the input galvanometer reading should not be too small for a desirable precision, the attenuator shown in Fig. 1 was used. This attenuator, of a ladder type, was constructed of very small high resistance wire. Its constant, calculated from d.c. voltage and resistance measurements, was $k = 0.00764 \pm 0.00001$.

The amplifier and shot circuit were in metal boxes inside a double walled wire cage. The oscillator and various parts of the input system were in separate metal boxes as shown in Fig. 1. Special shielding precautions were necessary since this type of input circuit is inherently sensitive to stray signals from the oscillator.

The tuned shot circuit was given additional protection by shortening the connecting wires and enclosing the inductance in a grounded copper box within the usual metal shot box.

Because of the presence of the attenuator, only a small fraction of the measured current through the input thermocouple eventually reaches the inductance potentiometer. Therefore any currents induced in the attenuator will produce relatively large errors in the potentiometer currents. Since the attenuator is of high impedance, these induced currents are inevitable unless it is well shielded from the coil delivering power from the oscillator. With the unshielded attenuator the input-output curve was not a straight line but a complicated curve not passing through the origin. The necessary shielding was accomplished by surrounding the attenuator with a brass cylinder closed at the attenuator end and extending for several inches over the end of the inductance potentiometer. This brass cylinder was insulated from the potentiometer and inner cage, and was connected to the outer cage.

A third source of stray signals is currents in the shielding metal near the zero end of the inductance potentiometer. These cause a signal on the amplifier when the oscillator is turned on with zero length of the potentiometer in use. Also, if signals are delivered to the amplifier varying l and keeping I_1 constant, the output will not be proportional to l^2. This error is especially serious since the undesired voltage bears a definite phase relation to the calibration voltage, so that correction may not be made by a subtraction of the initial deflection from the total amplifier output, as in the case of two independent voltages. With the squared output scale, an initial deflection of 2 mm in a total deflection of 200 mm may mean an error of 20 percent in the mean squared calibration voltage. It was

[6] A. W. Hull, Proc. I. R. E. **6**, 5 (1918).
[7] A. Russell, Phil. Mag. **17**, 524 (1909).

found that a stray signal of 4×10^{-9} volt would cause an error of 1 percent in the calculation of i_0 from (14) when i_0 was about 0.5 ma. This stray signal was sufficiently eliminated by making all the grounds of the amplifier and shot circuit, and of all the shielding inside the inner cage to the exact zero end of the inductance potentiometer. The tests of the effectiveness of this system of grounds were (1) that with $l=0$ no output deflection was observed with an amplification several times that necessary for measuring the shot effect; and (2) that for different values of l with I_1 constant, the outputs were proportional to l^2 within less than 1/2 percent.

The Experimental Procedure

During a series of measurements the effective plate resistance of the shot tube varies; this alters the equivalent series resistance R of the shot circuit. Although R does not appear explicitly in Eq. (14), an increase in R decreases the amplification at ω_0, and broadens the resonance curve, thus increasing both v_1^2 and A. The change in amplification at ω_0 is automatically measured whenever the calibrating voltage is applied; but to redetermine A for each experimental point is laborious and time consuming. It was desirable to make the measurements as quickly as possible since there were gradual changes in the sensitivity of the surfaces emitting secondary electrons. Hence A was predetermined once and for all as a function of the amplification at ω_0 over the whole range of resistance change introduced by the shot tubes. This was done by inserting small series resistances, 2.36 ohms to 16.6 ohms, in the resonant circuit. After the calibration it was only necessary to keep the filament currents and plate voltages of the amplifier constant with the aid of meters. A direct check of A from time to time showed the validity of this procedure. A was found to vary less than 0.2 percent with time.

The half-width of the amplification curve ranged from 1.5 to 2.8 kc, and the corresponding values of A from 1.75 to 2.98 kc.

The actual shot measurements were made in the following way. Conditions were chosen so that the shot effect to be measured gave an output deflection d_1 equal to approximately 1/2 full scale. Then a signal was introduced into the shot circuit from the inductance potentiometer such that the output deflection was approximately doubled, its value becoming d_2. Because of the random nature of the shot effect d_1 and d_2 were unsteady. A satisfactory procedure was to make ten readings of each at regular time intervals. For convenience, instead of attempting to make d_2 exactly equal to $2d_1$, the input current was slightly corrected to get the value of I_1 for use in Eq. (15). The filament circuit of the shot tube was then opened, and an output d_3 due to the calibrating voltage alone was obtained. The ratio $d_3/(d_2-d_1)$ gave the relative amplification necessary to obtain A from the curve previously prepared. It was necessary to leave a resistance in the shot circuit while measuring shot effects of secondary emission plate currents because of the negative resistance characteristic of the shot tube.

A test of the reliability of the apparatus and experimental procedure was made by evaluating e from the data on several temperature limited shot currents ranging from 0.2 ma to 1.0 ma. The values of e ranged from 1.570×10^{-19} to 1.604×10^{-19} coulomb, with an average of 1.587×10^{-19} coul. Calculation of the precision of e from Eq. (15), assuming very conservative values for the precisions of the various measured quantities gave a precision of ±1.5 percent. In the secondary emission measurements there was an added uncertainty due to the slight unsteadiness of the secondary emission. It is estimated that the precision of the J's was not worse than ±2 percent.

The Secondary Emission Tubes

The shot effect measurements on secondary emission were made on five three-element tubes designated A, B, C, D, E. The measurements on Tubes D and E were made with the resistance coupled amplifier. Tubes A, B and C were of type 201A, D and E of type 210. These tubes were sensitized for secondary emission by Mr. H. C. Thompson, except for Tube C, which was an ordinary factory tube. The material used for sensitization was BaO. The grid wires were of nickel, and the plate material was molybdenum

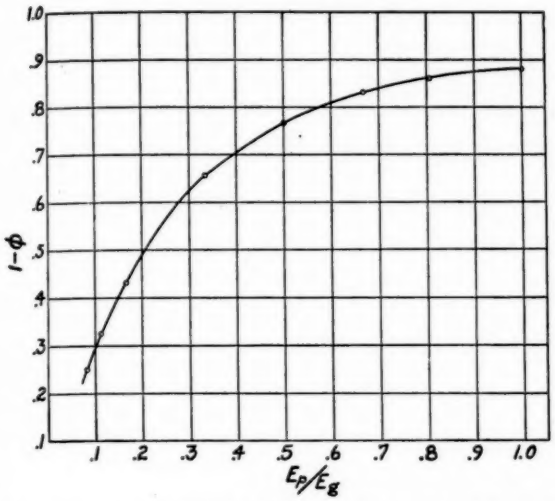

FIG. 2. Hyatt's values of $(1-\phi)$ as a function of E_p/E_g for a 201A tube. $E_g=360$ volts.

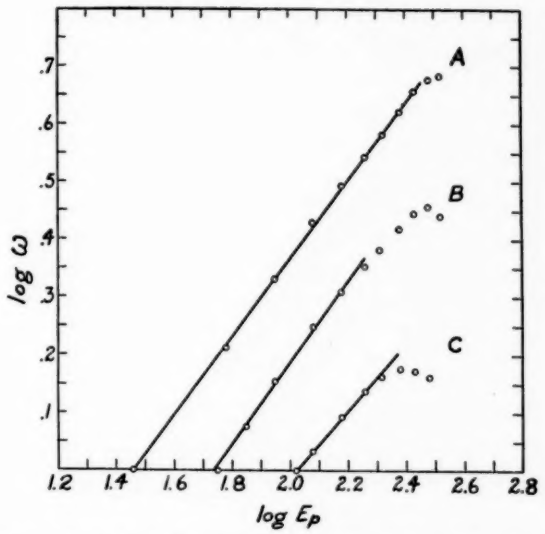

FIG. 3. Relation between log ω and log E_p for tubes A, B, and C.

or nickel. Typical plate voltage-plate current curves for similar tubes are shown by Hull.[6] In the tubes used secondary emission began at plate voltages between 5 and 10 volts. The plate current became zero ($\omega=1$) at voltages ranging from 20 to 124 volts. These values varied somewhat with the grid voltage. This is probably due to variations of angle of incidence of the primaries due to the geometry of the tube. At higher plate voltages the plate current became negative, and in some cases was over three times the total emission from the filament.

Although it is possible to tell from the plate current-plate voltage curves that at the high plate voltages several secondary electrons are emitted for each primary incident on the plate, it is impossible to calculate ω unless the fraction $(1-\phi)$ of the primary electrons which strike the plate is known. Since $(1-\phi)$ is a function of the relative grid and plate voltages, it must be measured experimentally. These measurements were kindly made for the author on a tube of type 201A by Dr. J. M. Hyatt, using the published[8] method of calibration with positive caesium ions. The curve showing the relation between $(1-\phi)$ and E_p/E_g for $E_g=360$ volts is shown in Fig. 2. This curve is decidedly different from the curves Hyatt obtained with a tube having cylindrical elements and an axial filament. In that case, for E_p/E_g from 0.1 to 2.0 the fraction of positive ions caught by the grid was found to agree closely with the ratio of solid to open portions of the grid. In the 201A type tube with closed flattened plate and grid and hairpin filament, the plate receives in general fewer electrons than would be predicted from the geometry. It should be noted, however, that the fraction striking the plate as E_p/E_g approaches 1 is 0.88, which agrees with the value 0.87 calculated from the dimensions of the grid wires and supports.

Fig. 3 shows the relation between log ω and log E_p for tubes A, B and C with $E_g=368$ volts. Lower values of E_g gave curves similar in shape but somewhat displaced to the right, corresponding to the slightly higher values of E_p for $\omega=0$. The curves are all characterized by a linear portion at the smaller values of E_p, and then a region where ω increases less rapidly, or even decreases as E_p increases. The maximum comes at higher voltages for the more sensitive tubes. All these tubes have the same geometry. It is certain that the falling off of ω at higher voltages is not due to space charge or to errors in ϕ.

The following equations hold for the linear portions of the curves for A, B, and C, respectively:

$$\omega_A=(E_p/29)^{.67};\ \omega_B=(E_p/54)^{.73};\ \omega_C=(E_p/105)^{.57}.$$

[8] J. M. Hyatt, Phys. Rev. **32**, 922 (1928); **33**, 1100A (1929).

Data obtained by Hyatt and Smith[9] and by Copeland[10] on heat-treated molybdenum when plotted in this way show similar curves. The straight portions yield exponents of approximately 0.34 and 0.44. Fröhlich[11] has derived relations between ω and E_p for the ends of the range of E_p. He finds that ω should increase in proportion to $E_p^{1/2}$ at low voltages, whereas when E_p is a few hundred volts, ω should decrease slowly with increasing E_p.

Results

Typical values of the secondary emission shot effects J_g and J_p are shown plotted against ω in Fig. 4. The units of the J's are, as stated above,

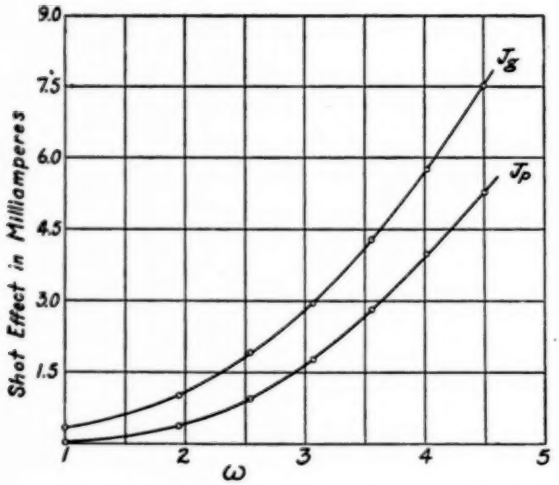

FIG. 4. Plate and grid shot effects as a function of ω, for tube A. $E_g=368$ volts. $i_0=0.303$ ma.

milliamperes of temperature limited shot current which would give the same fluctuations as the secondary emission currents. The curves shown are for tube A with $E_g=368$ volts. The curves for different grid voltages are similar, but not identical since ϕ is involved in the magnitudes of J_g and J_p. For tube B, which is a poorer secondary emitter, the curves are higher, while for tube E, the best emitter, the J values are lowest. Tubes C and D, for which measurements were made only at $\omega=1$, also follow this rule.

The first object of the secondary emission measurements was to decide between Eqs. (10)

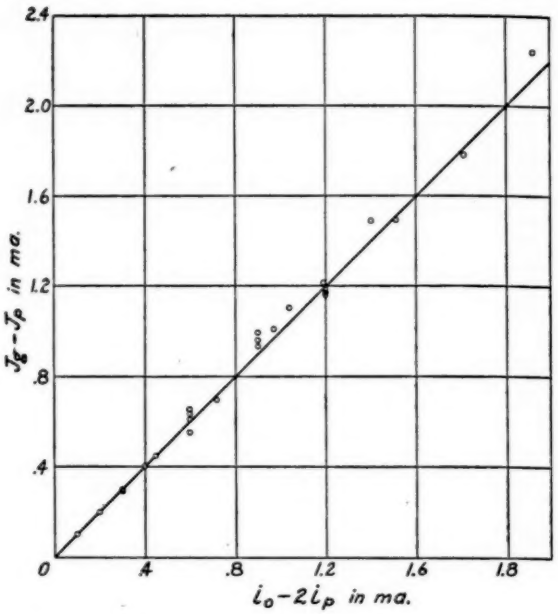

FIG. 5. J_g-J_p as a function of i_0-2i_p, for all tubes and voltages. The 45-degree line is the theoretical relation for the simultaneous case.

and (11). It was found that J_g was always larger than J_p, and hence Eq. (11) cannot hold. To verify Eq. (10) J_g-J_p has been plotted for all the observed experimental points against i_0-2i_p, Fig. 5. A 45° straight line representing Eq. (10) has also been drawn, and it is evident that most of the points lie on this line within the expected precision. For instance, the large deviation of the largest J_g-J_p is more than accounted for by assuming a 2 percent error for each of the J's.

In this figure a number of results are invisible because the value of i_p was zero, so that all such points would fall together on the curve. These points are shown separately in Table I. In this case Eq. (10) reduces to $J_g-J_p=i_0$. The last two columns show the agreement between these quantities. The discrepancies are on the average about 1 percent. The agreement is thus better than would be expected from the precision of the J's. This is due partly to the fact that the secondary emission was steadiest at the low plate voltages. Furthermore, since J_p was much less than J_g the magnification of errors arising from taking the difference was less serious.

The above data show definitely that primary impact and secondary emission are simultaneous within 10^{-6} second or less, since it is reasonable

[9] J. M. Hyatt and H. A. Smith, Phys. Rev. **32**, 929 (1928).
[10] P. L. Copeland, J. Frank. Inst. **215**, 593 (1933).
[11] H. Fröhlich, Ann. d. Physik **13**, 229 (1932).

TABLE I. *Summary of secondary emission shot effect measurements at $i_p=o$, $(\omega=1)$, showing the range of grid and plate voltage and also the verification of the relation $J_g-J_p=i_0$.*

TUBE	E_g (volts)	E_p (volts)	J_g (ma)	J_p (ma)	J_g-J_p (ma)	i_0 (ma)
A	368	28.5	0.357	0.0420	0.315	0.303
	319	30.5	0.349	0.0454	0.304	0.303
	184	32.0	0.381	0.0714	0.310	0.303
	138	33.5	0.395	0.0950	0.300	0.303
	92	35.0	0.440	0.137	0.303	0.303
B	368	56.0	0.395	0.0978	0.297	0.303
	184	58.0	0.476	0.169	0.307	0.303
C	368	108	0.503	0.193	0.310	0.303
	230	124	0.548	0.245	0.303	0.303
D	145	48	0.162	0.058	0.104	0.100
	145	48	0.302	0.107	0.195	0.200
	145	48	0.625	0.225	0.400	0.400
E	230	20	0.230	0.0274	0.203	0.200
	46.0	27.5	0.309	0.110	0.199	0.200
	46.0	27.5	0.311	0.111	0.200	0.200

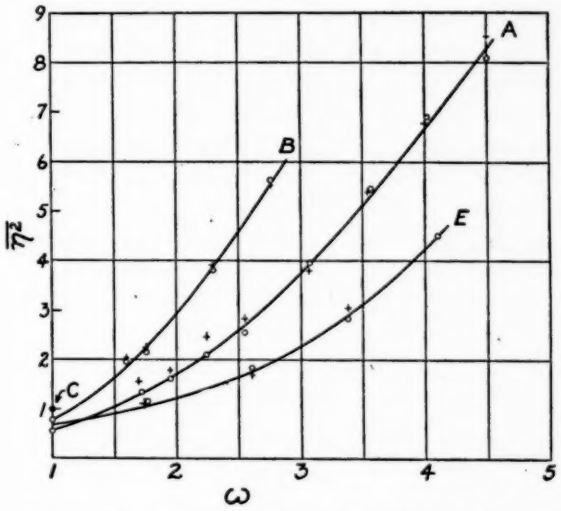

FIG. 6. $\overline{\eta^2}$ as a function of ω, for Tubes *A*, *B*, *C*, and *E*, and for all voltages. The circles refer to plate fluctuations and the crosses to grid fluctuations.

to expect that some deviation from the equation expressing simultaneity would appear if the average time between impact and secondary emission were one-tenth the period of the shot circuit.

The quantity $\overline{\eta^2}$ can be calculated from either J_p or J_g by Eqs. (12) and (13). This has been done for tubes *A*, *B*, *C*, and *E*, with Hyatt's values of ϕ. These do not apply directly to tube *E*, which is of the 210 type. However, the size and spacing of the grid wires are the same in the two tubes so that in the range of E_p/E_g where ϕ is nearly constant and equal to the geometrical ratio, the ϕ's should be the same. The additional precaution was used of keeping E_p/E_g constant at 0.598 for all values of ω during the measurements on tube *E*. The values of $\overline{\eta_p^2}$ and $\overline{\eta_g^2}$ plotted against ω are shown in Fig. 6.

Like the *J*'s from which they are computed, the values of $\overline{\eta^2}$ are larger for the poor secondary emitters. At $\omega=1$, $\overline{\eta^2}$ ranges from about 0.5 to 1 for the tubes used. The values of $\overline{\eta^2}$ in general increase more rapidly than ω. The fact that $\overline{\eta_p^2}$ is somewhat different from $\overline{\eta_g^2}$ in the lower portions of the curves is again due to the multiplication of errors arising in the computation of $\overline{\eta_g^2}$. The values of $\overline{\eta_p^2}$ are considered much more reliable. The curves in Fig. 6 include measurements made with various grid voltages.

The relation between $\overline{\eta^2}$ and E_p is linear within the experimental precision for a given tube and grid voltage. The slope and intercept of the line vary with E_g and are also different from tube to tube.

DISCUSSION OF THE RESULTS

Theoretically the probable time interval between primary impact and secondary emission can be estimated in several ways. The comparison of computed and measured conductivities of metals leads to the conclusion that the mean free path of an electron entering a metal is of the order of 100 atom diameters.[12] This means that an electron entering a metal with 100 volts energy will lose its excess energy and become a member of the normal Fermi distribution in a time of the order of 10^{-14} second. The time interval between primary and secondary electron should be of this order of magnitude also.

Another estimate comes from the time during which the incident electron may be expected to stay in an excited level inside the metal (neglecting collisions). The probability of an electron transition to a given lower level in a metal should be of the same order as that for a similar transition in an atomic system. Because of the enormous number of available energy states in the

[12] A. Sommerfeld and H. Bethe, *Handbuch der Physik*, second edition, Vol. 24/2, p. 354.

metal, lifetimes of the order of magnitude given above should result.

It is therefore not surprising that the results indicate simultaneity, and some other explanation must be found to account for the result of Hull and Williams.

It is of interest to examine what would be expected theoretically for $\overline{\eta^2}$. To do this it is necessary to consider the known facts of secondary emission produced by primary electrons of several hundred volts energy.[13, 14, 15]

(1) At all incident energies there are some secondary electrons which have velocities nearly equal to that of the primaries. These are equivalent to reflected electrons, and there can be only one of them produced by any one primary. If such electrons are produced by a fraction x of the primaries, the value of ω for this fraction is equal to 1. Their contribution to the plate shot effect is zero. The value of x may be expected to depend on the nature of the surface and on the speed of the primaries. From the papers of Farnsworth[14] it appears that for moderately clean, pure metal surfaces x varies from 0.5 or more for 10-volt primaries down to a few percent for 100-volt primaries; and that x may be even greater for surfaces having adsorbed gas layers.

(2) There are some primaries which produce no secondaries because they communicate all their momentum to ions in the metal (inelastic collisions), or to electrons which are directed inward, or to electrons whose outward velocity component is not sufficient to carry them out through the surface. The number of these primaries will thus depend on the velocities and angular distribution of the secondaries inside the metal. Both factors may themselves depend on the energy of the primaries. Scattering of primaries and secondaries must be taken into account. All these considerations make the estimate of this fraction very difficult. If it is assumed, however, that the metal atoms scatter both primaries and secondaries like elastic spheres, the chances are relatively small that no secondaries would get out. Let the fraction of primaries which produce no secondaries be y. Then $\omega_y=0$; and the contribution to the plate shot effect, J_y, is that of an equivalent temperature limited current.

(3) Of the remaining primaries, some will produce many secondaries, some few. If this fraction is z, then $J_z=[(1-\omega_z)^2+\overline{\eta_z^2}]$. The range of values which ω_z and $\overline{\eta_z^2}$ may assume is predictable. Since each secondary loses an energy equal to or greater than the work function on its way out of the metal, the maximum number of secondaries which can be produced by any one primary is $(E_1+a)/(E_2+a)$, where a is the work function, E_1 the primary energy, and E_2 the average secondary energy, all in volts. If $a=3$ volts for the BaO surfaces used in this work, and $E_2=4$ or 5 volts from the data of Farnsworth, the maximum number becomes 3 to 40 for primary energies from 20 to 300 volts. There may also be as few as one secondary per primary. The cases in which this happens cannot be distinguished from cases of reflection except by experiments on velocity distribution such as those of Farnsworth[14] and Soller.[15]

The quantity $\overline{\eta_z^2}$ may have any value from zero to ω_z^2, depending on the distribution of the number ejected about the mean value ω_z. It can be shown that neither of these values will fit the data for any possible values of x, y, and z. Because of the large number of random factors involved in the secondary emission process, the most likely assumption is that the number ejected varies in purely random fashion. In this case $\overline{\eta_z^2}$ would be approximately equal to ω_z itself, at least for high primary voltages.

It is now necessary to derive the relation between ω_z and $\overline{\eta_z^2}$ and the ω and $\overline{\eta^2}$ of Campbell's less detailed picture. For unit primary current,

$$y+z(1-\omega_z)=1-\omega$$

or

$$\omega_z=(a+\omega-1)/z \quad \text{if} \quad (y+z)\equiv a, \qquad (16)$$

then

$$J_p=\{y+z(1-\omega_z)^2+\overline{\eta_z^2}\}=(1-\omega)^2+\overline{\eta^2}. \qquad (17)$$

Putting in $\overline{\eta_z^2}=\omega_z$ and the value of ω_z from (16),

$$\overline{\eta^2}=\omega(1-\omega)+(a+\omega-1)^2/z. \qquad (18)$$

It is therefore possible to determine certain limits for a and z from the experimentally obtained values of ω and $\overline{\eta^2}$. First of all, when

[13] W. Bothe, *Handbuch der Physik*, first edition, Vol. 24, p. 57.
[14] H. E. Farnsworth, Phys. Rev. **20**, 358 (1922).
[15] T. Soller, Phys. Rev. **36**, 1212 (1930).

$\omega=1$, Eq. (18) becomes $a^2/z=\overline{\eta^2}$, or as an upper limit $a=\overline{\eta^2}$. For tube A this would mean 40 percent reflected electrons, since $\overline{\eta^2}=0.6$; for the less sensitive tubes B and C, a would be higher. The reason why at $\omega=1$ there is less reflection for the less sensitive tubes is that the primary voltage is higher. These results are in agreement with the data of Farnsworth and of Soller.

For large values of ω, $(a-1)$ will be small compared to ω. Eq. (18) then gives

$$\overline{\eta^2}=\omega+\omega^2(1/z-1).$$

The data for the highest value of ω for each tube then lead to $z=0.96\pm0.01$ for tube E; $z=0.82\pm0.04$ for tube A, and $z=0.5\pm0.2$ for the tube B. In the latter case, the largest value of ω was only 2.8, so that the assumption $(a-1)\ll\omega$, is not good. In the middle ranges of ω little can be said of the parameters a and z.

The fact that at high primary energies z is so large for some tubes shows (1) that there is very little reflection, and (2) that there must be considerable scattering; for otherwise most of the secondaries would receive inward momenta, and the fraction y would be large.

The author takes pleasure in acknowledging her great indebtedness to Dr. A. W. Hull, who suggested this research and who contributed valuable suggestions and advice throughout the progress of the work. She also wishes to express her appreciation to Dr. J. M. Hyatt for the measurements of ϕ, and to Professor Bernhard Kurrelmeyer for assistance in taking the data and for discussion during the preparation of the paper.

Note added in proof August 23, 1935. In recent work the author has found that the variation of ω with grid voltage, observed throughout this work, is probably due mainly to secondary electrons from the grid, a few of which will have sufficient energy to reach the plate. Such electrons may also increase the grid and plate shot effects by amounts of the order of ten percent at the higher plate voltages. The relation $J_g-J_p=i_0-2i_p$ should remain accurately valid. The effects due to grid secondary electrons will be discussed in detail in a future paper.

The Effect of Changes in the Equilibrium Relative Vapor Pressure Upon the Capillary Structure of Wood*

ALFRED J. STAMM, *Forest Products Laboratory,† U. S. Department of Agriculture, Madison, Wisconsin*

(Received June 26, 1935)

Measurements have been made of the equilibrium permeabilities of softwoods to air of different relative vapor pressures. Transverse sections less than the average fiber length in thickness, in which the open cavities account for practically all of the permeability, show practically no change in permeability with changes in the equilibrium relative vapor pressure. Sections thicker than the maximum fiber length, the permeabilities of which are dependent upon the size of the pit openings, show an increase in permeability with a decrease in equilibrium relative vapor pressure. When the square root of the permeability is plotted against the moisture content of the wood in equilibrium with the various relative vapor pressures of air, practically a linear relationship is obtained from 0 to 20 percent moisture content. At higher moisture contents the permeabilities are considerably less than the linear relationship calls for. This is due to films of water forming across the capillaries. Higher pressures than those used are required to overcome the effect of the surface tension of the water in these capillaries. A new means of determining the distribution of size of openings in a porous membrane based on these findings is given.

THE capillary structure of wood has been studied from the pulping standpoint by Johnston and Maass[5] and by Sutherland, Johnston, and Maass,[13] and from the preservation standpoint by Buckman, Schmitz and Gortner.[2] The author has determined the effective capillary sizes in water-saturated wood by a combination of pressure permeability and electro-osmotic flow measurements.[7, 8] Electrical conductivity measurements[9, 10] that were also used have since been shown to be incapable of giving capillary sizes because of the erroneous assumption that the conductivity of the cell walls is negligible.

The only available data to give an indication of the effect of shrinking and swelling of wood upon the effective capillary sizes are those of Buckman, Schmitz and Gortner[2] which indicate that the effective capillaries increase in size upon drying of the wood. More complete information along this line should be of considerable value in determining and understanding seasoning, preservation, and pulping practice.

EXPERIMENTAL PROCEDURE

The equilibrium permeability of wood sections to air of different relative vapor pressures was measured with a modification of the differential pressure drop apparatus previously described (see Fig. 1).[8] It consists essentially of three compartments, 1 and 2 separated by the wood section and 2 and 3 separated by the standard capillary tube *C*. Manometers were provided to determine the pressure drop between compartments 1 and 2 and 2 and 3. The means of holding the sections was modified as follows: Holes were drilled in one end of cylindrical pieces of wood *W* in the fiber direction with a centerless bit, the bottom serving as a transverse section. A soft rubber stopper *R* connected the section to the apparatus. It showed no tendency to loosen or exert an appreciable stress on the section over a complete moisture change cycle. The wood section was enclosed in a large cylindrical glass tube with rubber stoppers at each end. A stopcock *S* was provided in compartment 2 to prevent the passage of air through the wood section during the course of bringing it to moisture equilibrium. This was done to cause humidification to occur from the outside of the specimen so as to more nearly duplicate normal drying and reabsorption conditions. An electric heating coil was wrapped about the exit tube *B* to prevent condensation of water from air at a high relative vapor pressure when being discharged from the apparatus. The apparatus was held at a temperature of 40°C in a thermostatically controlled water bath. The air was humidified by bubbling through saturated salt solutions in glass jars filled with glass beads. About an inch of mercury was placed in the bottom of the jars and the air first bubbled through this to prevent salt from working back into the jet. The air passed through a trap filled

* Presented before the Colloid Division, American Chemical Society, at its 89th meeting in New York City, April 22–26, 1935.

† Maintained at Madison, Wis., in cooperation with the University of Wisconsin.

with glass wool to remove any traces of entrained spray before entering the apparatus. The relative vapor pressures given in Table I were obtained from gravimetric determinations of the moisture content of the air at approximately the same rate of flow as that used in the experiments.

This apparatus proved satisfactory for determining the permeability of transverse sections. It could not be used, however, for radial and tangential flow as practically all the air would pass through the end-grain part of the cylindrical wall of the wood section rather than through the end. In the case of the transverse sections the passage of air through other than the end-grain ends was entirely negligible (1 percent or less). Further, this glass apparatus could not be used for other than the transverse sections because it would not stand the pressures required for obtaining measurable permeabilities with some of the resistant sections. It was thus necessary to devise another means of making the measurements using a more rugged apparatus.

It was found that sections clamped in the old type of flush rubber-gasketed flange, when carefully marked, could be removed from the clamp and reinserted in practically the same position with a variation in the pressure drop readings of not more than 2 to 3 percent. It was hence decided to use this type of flange clamp and remove the sections and prehumidify them to approximately the equilibrium relative vapor pressure of the air to be used in the next permeability test. In this way checking of the sections was entirely avoided. Although the source of error in these measurements was somewhat greater than in those made with the apparatus of Fig. 1, there was the distinct advantage of being able to make measurements on one series of sections while another series was being prehumidified.

TABLE I. *Relative vapor pressures obtained with different saturated salt solutions.*

MATERIAL	TEMPERATURE	RELATIVE VAPOR PRESSURE
	°C	
Distilled water	40	96.3
Saturated $BaCl_2$	40	86.7
Saturated NaCl	40	73.4
Saturated $MnCl_2$	40	50.5
Saturated $MgCl_2$	40	31.0
Saturated LiCl	40	11.7
P_2O_5	40	0.0
Distilled water	23–25	98.0
Saturated $BaCl_2$	23–25	89.3
Saturated NaCl	23–25	74.5
Saturated $MgCl_2$	23–25	31.0
P_2O_5	23–25	0.0

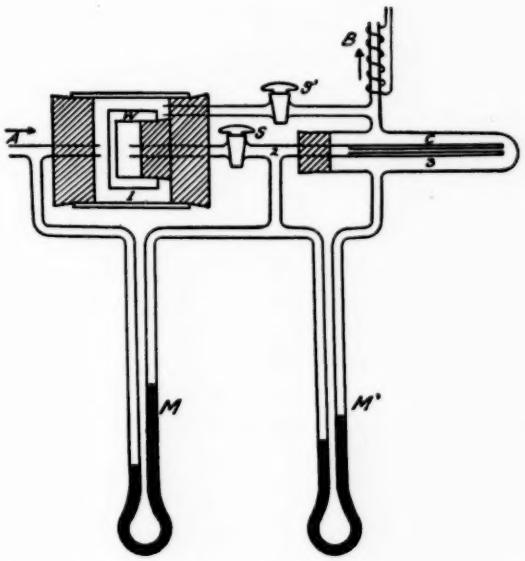

FIG. 1. Low pressure permeability apparatus used for making measurements on transverse sections of wood.

More substantial humidifiers were also necessary for these measurements. They were made of galvanized iron pipe with fritted glass disks clamped to the lower end of the pipe to break up the air into fine bubbles. To prevent the salt from clogging the fritted glass disks, air was always passed through a water prehumidifier first. The salt solutions thus always reduced the relative vapor pressure of the air rather than raised it. These humidifiers were used only at room temperature, 23° to 25°C. The relative vapor pressures obtained with them are given in Table I. The sections were prehumidified in humidity rooms held at 80°F and 30, 75, 90 and 97 percent relative humidity, respectively, and in a desiccator over P_2O_5 for at least a week. The equilibrium relative vapor pressure change in the apparatus was so small that readings could be made as quickly as pressure equilibrium was established.

The velocity of the flow of air through both the standard capillary tube and the wood sections can be expressed by Poiseuille's equation:

$$V_c = \pi r_c^4 P_c / 8\eta l_c \quad \text{(for standard capillary tube } c\text{)}, \quad (1)$$

$$V_w = NQ\pi r_w^4 P_w / 8\eta l_w \quad \text{(for the wood section)}, \quad (2)$$

in which V_c and V_w are the velocities of flow through the capillary and through the wood section, r_c and r_w are the radius of the capillary and the average effective radius (to be more exact, the fourth root of the average fourth power) of the wood capillaries, l_c and l_w are the corresponding lengths and P_c and P_w the corresponding pressure drops, η the viscosity of the air, N the number of effective capillaries in the wood sections in parallel per unit of cross section and Q the effective cross section, all expressed in centimeter-gram-second units. When the standard capillary and the wood section are connected in series as in this investigation

$$V_c = V_w \tag{3}$$

and

$$Nr_w^4/l_w = r_c^4 P_c/Ql_c P_w. \tag{4}$$

Both N and r_w are unknown so that in order to determine either, further data are necessary.[8, 9] During the course of the shrinking and swelling of wood, N will, however, remain constant unless checking occurs. The pressure drop ratio P_c/P_w and the standard pressure drop ratio $r_c^4 P_c/Ql_c P_w$ should thus be proportional to the fourth power of the capillary radii. The change in size of the capillary openings in wood have hence been expressed in terms of the pressure drop ratio in this investigation.

Experimental Results

Measurements of the pressure drop ratio for thin transverse sections less than a fiber length in thickness of the heartwood of initially green western hemlock and air-dry white pine at different equilibrium relative humidities are shown in Table II. Air was passed around the outside of the sections and out through stopcock S' (Fig. 1) for two days before passing it through the section in order to bring them to equilibrium with the vapor pressure of the air. Pressure drop readings were then made over a period of two days. The total pressure drop used was never greater than 20 cm of water. The data show that the fiber cavities change but very slightly in size with shrinking and swelling of the wood. The mean deviation of the effective capillary radius for the white pine was about 0.5 percent and for the western hemlock specimens still less. In the case of the white pine a part of the permeability

Table II. *Effect of changes in relative vapor pressure upon the permeability of transverse sections of wood less than a fiber length in thickness.*

Species	Dimensions of sections		Capillary constant r_c^4/l_c	Relative vapor pressure of air	Equilibrium pressure drop ratio	Mean deviation
	Thickness	Cross section				
	Cm	*Cm²*				*Percent*
White pine heart	0.22	1.37	1.85×10^{-8}	0.963	1.96	
				.867	2.04	
				.734	2.05	
				.505	2.08	
				.310	2.10	
				.117	2.08	
				.000	2.02	
				.117	2.00	
				.310	2.05	
				.734	1.99	
				.963	1.95	2.01
Western hemlock heart	.22	5.30	1.47×10^{-7}	.734	9.50	
				.505	9.50	
				.310	9.69	
				.117	9.55	
				.000	9.88	
				.117	9.62	
				.310	9.77	
				.505	9.68	
				.734	9.53	
				.867	9.63	
				.963	9.67	.94
Western hemlock heart	.40	5.30	1.47×10^{-7}	.963	2.89	
				.867	2.84	
				.734	2.86	
				.310	2.84	
				.117	2.93	
				.000	2.96	
				.117	2.96	
				.310	2.98	
				.505	2.94	
				.734	2.90	
				.867	2.89	1.43

may have been through resin ducts. These are entirely absent from western hemlock so that the permeability of these sections was entirely through open fiber cavities. This approximate constancy of the size of the fiber cavities is in agreement with findings of Schwalbe and Beiser[6] and Beiser,[1] and with the density-shrinkage relationships for small sections of wood dried under as nearly stress-free conditions as possible developed by the author.[11]

Similar measurements were made on initially green transverse sections of both the sapwood and the heartwood of western hemlock greater than the maximum fiber length in thickness. The results obtained for several relative vapor pressure change cycles are shown in Fig. 2. The curves are numbered in order and the desorption part of the cycle indicated with open circles and the adsorption part with black circles. There is a definite increase in the pressure drop ratio with decreasing equilibrium-relative vapor pressure indicating that the effective capillaries in the pit membranes increase in size when the wood shrinks. During the first cycle true equilibrium was not obtained or a slight checking of the sections occurred. After this the relative vapor pressure cycles were quite reproducible. Adsorption values of the pressure drop ratio were in all cases slightly greater than the corresponding desorption values. These hysteresis loops are entirely comparable with those for the moisture content-relative vapor pressure[12] and electrical conductivity-relative vapor pressure relationships.[14] The electrical conductivity-moisture content relationship calculated from the relationships of each with the relative vapor pressure gives a relationship free from hysteresis effects. The same is true when the pressure drop ratio-relative vapor pressure relationship is converted to a pressure drop ratio-moisture content relationship basis. The pressure drop ratio is proportional to the fourth power of the effective radius (see Eq. (4)). The square root of the pressure drop ratio is hence proportional to the effective cross-sectional area of the capillaries. The relationship between the square root of the pressure drop ratio and the equilibrium moisture content is plotted in Fig. 3 for the same data as in Fig. 2. A linear relationship free from hysteresis effects is obtained below a moisture content of approximately 20 percent. The external volumetric and cross-sectional swelling of wood is directly proportional to the moisture content from oven-dry to the fiber-saturation point.[11] The cross-sectional areas of the pit membrane openings thus appear to be inversely proportional to the extent of swelling of the membranes. Evidently the thin pit membranes respond to changes in the relative vapor pressure more rapidly than does the relatively heavy rim about the membrane. In the course of desorption the membrane tends to shrink on drying. As the response of the heavy rim is considerably slower the membrane is put under tension. This tension is relieved by internal shrinkage which results in an increase in the cross section of the openings.

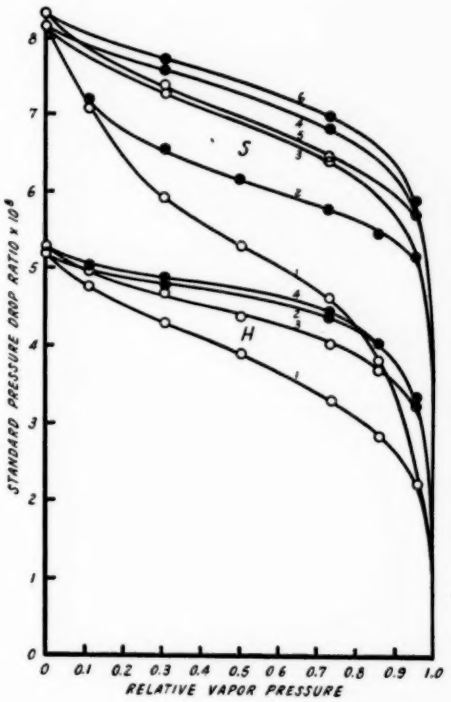

FIG. 2. Effect of changes in the relative vapor pressure of air passing through transverse sections of the heartwood and the sapwood of western hemlock upon the resulting equilibrium pressure drop ratio. Numbers indicate order of measurements: Open circles, desorption; closed circles, adsorption.

Similar determinations of the relationship between the moisture content and the square root of the equilibrium pressure drop ratio were made on sections of both seasoned white pine heartwood and initially green heartwood and sapwood

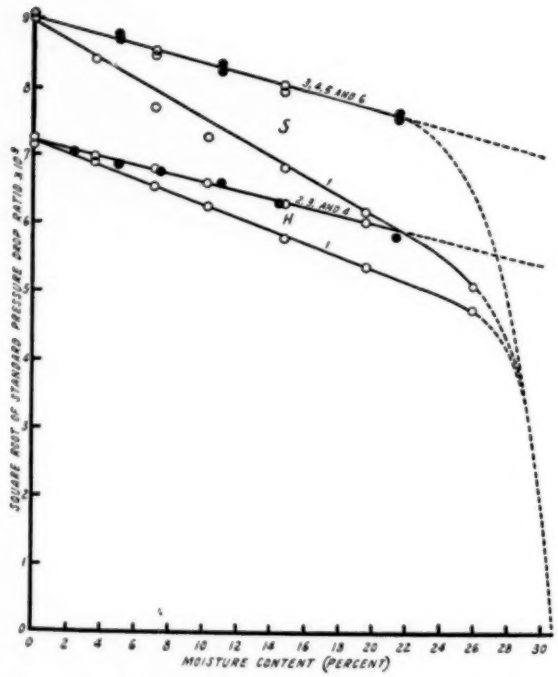

FIG. 3. Effect of changes in the moisture content of transverse sections of the heartwood and the sapwood of western hemlock upon the square root of the equilibrium pressure drop ratio. Numbers on curves refer to those of Fig. 2. Open circles, desorption; closed circles, adsorption.

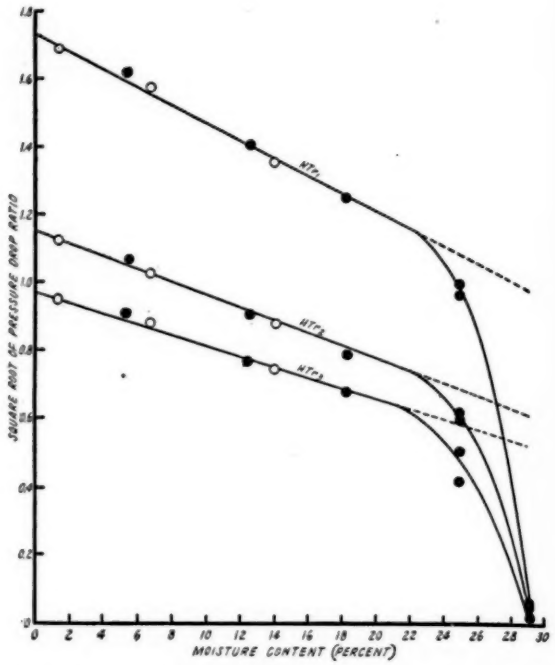

FIG. 4. Effect of changes in the moisture content of transverse sections of the heartwood of white pine upon the square root of the equilibrium pressure drop ratio. Open circles, desorption; closed circles, adsorption.

of western hemlock cut in the three different structural directions using the second apparatus.

The measurements were made with total pressure drops ranging from 5 to 100 cm of mercury for the different sections. Readings at at least three different pressures were taken with each section. The pressure drop ratio P_c/P_w was plotted against the total pressure drop P_c plus P_w and the value of P_c/P_w extrapolated to zero applied pressure was used in the calculations. This graphically corrects for impact turbulence effects.[8] The pressure drop ratios built up to a maximum and then decreased to an equilibrium value which was used in these calculations. This effect for the vapor flow was considerably less than that reported by Buckman, Schmitz and Gortner[2] for liquid flow as might be expected for electrokinetic effects would undoubtedly be less for vapor flow than for liquid flow.

The results of these measurements with the second apparatus are given in Figs. 4, 5, and 6. In all cases the square root of the pressure drop ratio increases in a linear manner with a decrease in the moisture content from about 20 percent to oven dry. Further, the ratio of the square roots of the pressure drop ratios at 0 percent and 20 percent moisture content are practically constant for sections of different thickness and even for sections cut in the different structural directions, but the values seem to vary with the species. The values of this ratio are given in Table III together with the thicknesses of the sections and the standard pressure drop ratio for unit effective thickness. The measurements made by the first method are for a varying cross section caused by shrinking and swelling of the section. The measurements made by the second method are for a fixed cross section determined by the size of the opening in the flange. As the wood shrinks the number of capillaries that are effective for flow increases. For this reason the ratios of the square roots of the pressure drop ratios obtained by the second method are higher than those obtained by the first. The values obtained by the second method were corrected to the basis of the first by dividing by 1 plus the cross-sectional shrinkage from 20 to 0 percent moisture content (see last column of Table III).

These ratios of the square roots of the equi-

librium pressure drop ratios seem to depend upon the nature of the membranes traversed rather than the arrangement and number traversed in series or parallel. If the pit membranes which are composed of lignin have a similar hygroscopicity to that of the wood as a whole, which seems to be the case, the volumetric shrinkage of the membrane substance from 20 to 0 percent moisture content should be about 20 percent. If it is assumed that the rim of the membrane changes dimensions by a negligible amount during the course of the shrinkage of the membrane, hypothetical values for the ratio of the square roots of the pressure drop ratios for 0 and 20 percent moisture content can be calculated for various specific cases. If the shrinking manifests itself entirely as a change in the thickness of the membrane, the ratio would be 1.12. If the shrinkage of the membrane manifests itself entirely by increasing the size of the openings in the plane of the membrane, the value of the ratio would depend upon the fractional void cross section of the membrane. If this were one-half, the ratio would be 1.20, if one-quarter, the ratio would be 1.40. In reality there is very likely a change in both the thickness of the membrane and in the size of the openings. If one-half of the shrinkage manifests itself in the direction of the thickness of the membrane and the other half in the plane of the membrane and the void cross section of the membrane is one-quarter, then the ratio of the square roots of the pressure drop ratios will be 1.26. This hypothetical value is in reasonable agreement with the actual experimental values.

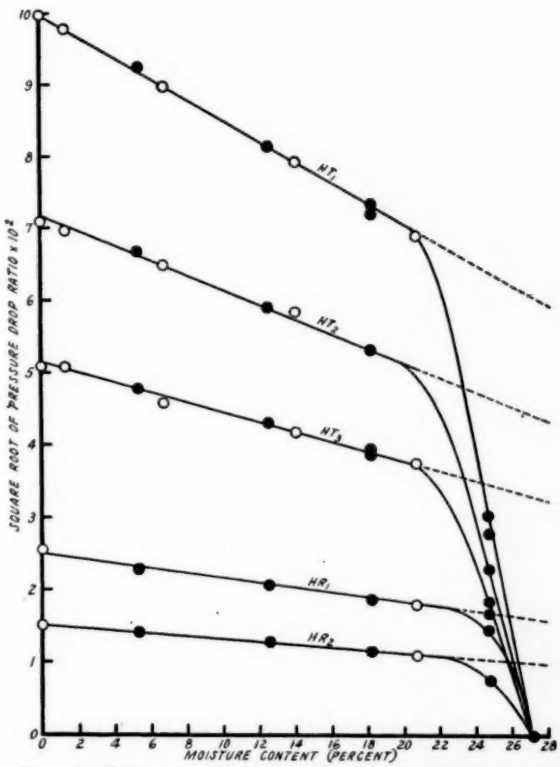

FIG. 5. Effect of changes in the moisture content of tangential and radial sections of the heartwood of white pine upon the square root of the equilibrium pressure drop ratio. Open circles, desorption; closed circles, adsorption.

TABLE III. *Changes in permeability of wood with changes in thickness and moisture content.*

SPECIES (1)	KIND OF SECTION (2)	SECTION NO. (3)	THICKNESS OF SECTIONS (4)	STANDARD PRESSURE DROP RATIO FOR EFFECTIVE UNIT THICKNESS OF DRY WOOD (5)	RATIO OF THE SQUARE ROOTS OF THE PRESSURE DROP RATIOS FOR DRY WOOD AND WOOD AT 20% MOISTURE CONTENT (6)	COLUMN (6) CORRECTED FOR EXTERNAL SWELLING (7)
			Cm			
Western hemlock	Sap transverse	[1]0	1.300	8.15×10^{-8}	1.175	1.175
	Heart transverse	[1]0	1.310	5.25×10^{-8}	1.200	1.200
		1	.919	1.26×10^{-8}	1.282	1.176
		2	1.857	1.18×10^{-8}	1.302	1.193
		3	2.880	1.14×10^{-8}	1.288	1.180
	Sap tangential	1	.184	5.57×10^{-13}	1.215	1.153
		2	.189	1.79×10^{-13}	1.230	1.168
	Sap radial	1	.186	9.50×10^{-12}	1.233	1.197
	Heart tangential	1	.196	4.58×10^{-13}	1.245	1.177
	Heart radial	1	.169	6.29×10^{-13}	1.222	1.183
White pine	Heart transverse	1	1.148	4.13×10^{-9}	1.420	1.322
		2	2.125	3.78×10^{-9}	1.475	1.373
		3	2.980	3.85×10^{-9}	1.475	1.373
	Heart tangential	1	.158	2.45×10^{-12}	1.400	1.330
		2	.202	1.56×10^{-12}	1.385	1.315
		3	.255	1.03×10^{-12}	1.368	1.300
	Heart radial	1	.112	1.10×10^{-13}	1.365	1.335
		2	.140	5.00×10^{-14}	1.352	1.322

[1] These measurements were made with the first apparatus; r_c^4/l_c was 3.73×10^{-9} and the effective cross section 1.37 cm². The other measurements were made with the second apparatus; r_c^4/l_c was 5.27×10^{-10} and the effective cross section 0.353 cm².

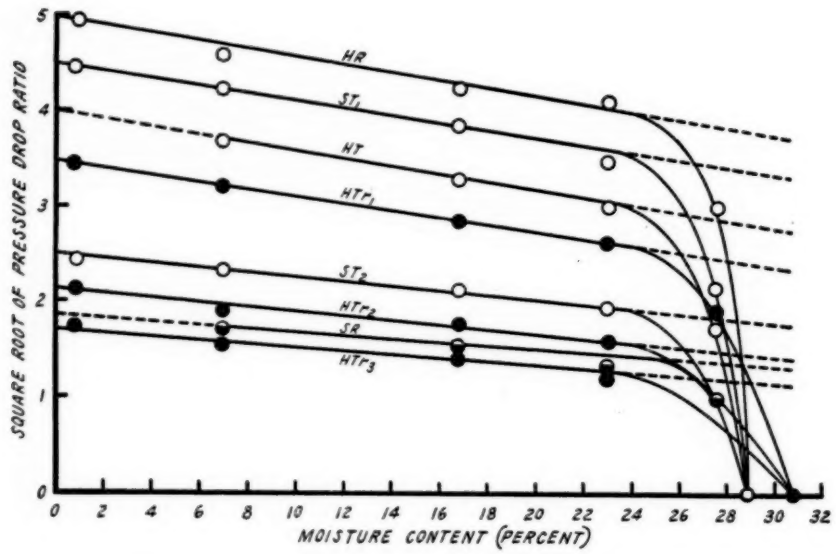

FIG. 6. Effect of changes in the moisture content of transverse, tangential, and radial sections of both the heartwood and sapwood of western hemlock upon the square root of the equilibrium pressure drop ratio. All desorption curves. Open circles, ordinates as given; half-circles, 10× ordinates; closed circles, 100× ordinates.

If the capillary structure of wood were quite uniform the standard pressure drop ratios per unit of effective thickness should be fairly constant for each structural direction. This is only approximately true in the fiber direction and not at all true in the other directions (Table III). All the measurements made on transverse sections were for sections only a few fiber lengths in thickness. The effective thickness of these sections is hence appreciably less than the actual thickness as air passing through the sections traverses on the average one-quarter of an open fiber length at each end. The number of pit membranes traversed in series is hence approximately proportional to the thickness of the section minus one-half of the average fiber length (0.17 cm). This effective thickness was used in the calculations of the standard pressure drop ratio per unit effective thickness for the transverse sections. The number of membranes traversed in series for the other sections was so great that the difference between actual and effective thickness was negligible. The standard pressure drop ratios per unit of effective thickness decrease somewhat with increasing thickness even for the transverse sections. This is due to the fact that the probability of maximum-sized openings occurring in series decreases with an increase in the number of membranes traversed in series. It can be readily demonstrated that the permeability is greater if the maximum-sized openings occur in series rather than when they occur in parallel.

The data show an appreciable deviation from the linear moisture content-square root of the pressure drop ratio relationship at moisture contents exceeding 20 percent. The square roots of the pressure drop ratios are less than the linear relationship calls for. This is due to the fact that moisture condenses in part of the effective capillaries even below the equilibrium saturation pressure because of their minute size and eliminates them as a source of flow. The relationship between the curvature of a drop and its equilibrium vapor pressure is given by Kelvin's equation

$$r = 2\sigma M/\rho RT \ln p_0/p, \qquad (5)$$

in which r is the radius of the drop or of the capillary in which it forms, p_0 is the saturation vapor pressure at the absolute temperature T, p is the vapor pressure over the drop or liquid in the capillary, R is the gas constant, σ is the surface tension of the liquid, M the molecular weight, and ρ the density, all expressed in centimeter-gram-seconds. The relative vapor pres-

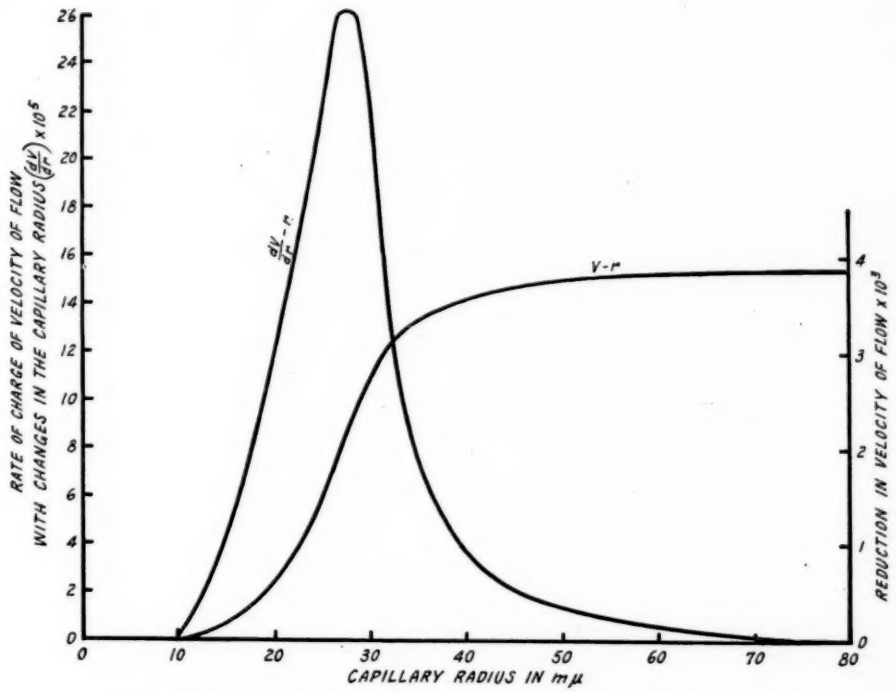

FIG. 7. Distribution of the size of the capillaries effective in controlling the flow of air in a tangential section of white pine (T_1).

sure in equilibrium with the moisture content at which the deviation from the linear relationship begins is practically 0.9 for all of the curves. This corresponds to a capillary radius of 10 mμ. It is slightly less than the average effective capillary radius previously determined by the electro-osmotic method.[8] At moisture contents in equilibrium with higher and higher relative vapor pressures more and more of the capillary structure is obstructed due to condensation of films of water that cannot be broken at the pressures under which the measurements were made. Measurements were also made of the pressure required to overcome the effect of surface tension of water in the saturated sections using the second apparatus. This proved to be more sensitive to the detection of the initial flow of air than the method previously used. For all the transverse sections, detectable displacement of water by air occurred at lower pressures than previously reported.[8] These pressures in the case of the transverse white pine sections were less than the maximum operating pressures used in making the measurements on the same sections at lower moisture contents (15 to 20 cm of mercury). Finite values of the square root of the pressure drop ratio were hence obtained at the saturation moisture content of 29 percent (Fig. 4). In the case of the transverse sections of western hemlock (Fig. 6) the pressures required to overcome the effect of surface tension ranged from 0.5 to 2 kg per square centimeter. Although these values exceed the pressures used in the measurements, the corresponding capillary sizes, 70 to 2800 mμ, are so large that the vapor pressure depression by them is less than 0.1 percent. The square root of the pressure drop ratio will thus be zero at practically the saturation moisture content (30.7 percent). In the case of the tangential and radial sections of both species the pressure required to overcome the effect of surface tension ranged from 20 to 25 kg per square centimeter, corresponding to capillary sizes of 75 to 60 mμ, and relative vapor pressures of 98.6 to 98.2 percent. These correspond to moisture contents of 27.2 percent for the white pine and 28.9 percent for the western hemlock.

The distribution of size of the capillaries effective in controlling the rate of flow of air can be calculated from the deviations from the linear

moisture content-square root of the pressure drop ratio relationship. The deviation of the pressure drop ratio or velocity of flow from the theoretical value at different moisture contents in equilibrium with various relative vapor pressures was converted to a pressure drop change-capillary radius basis with the use of Eq. (5) for a tangential section of white pine. The values are plotted in Fig. 7, together with the distribution curve which was obtained by graphically determining the slope of the former curve. Sufficient experimental values for the pressure drop ratio at different equilibrium relative vapor pressures were not obtained to determine the distribution curves with any certainty but the example given gives the general nature of the curve. The most probable radius and average radius are practically the same and have a value of about 28 mμ. This value is but slightly larger than the average values previously obtained by combining electro-osmotic data and pressure permeability data.[8]

This method for obtaining the distribution of size of pores should be applicable for all kinds of membranes in which the openings are sufficiently small to appreciably reduce the relative vapor pressure. In the case of nonswelling membranes the linear part of the relationship would, of course, be parallel to the abscissa axis.

References

[1] W. Beiser, Kolloid Zeits. **65**, 203 (1933).
[2] S. J. Buckman, H. Schmitz and R. A. Gortner, J. Phys. Chem. **39**, 103 (1935).
[3] J. Duclaux and J. Errera, Rev. Gen. Colloides **2**, 130 (1924).
[4] D. I. Hitchcock, J. Gen. Physiol. **9**, 755 (1926).
[5] H. W. Johnston and O. Maass, Can. J. Research **3**, 140 (1930).
[6] C. G. Schwalbe and W. Beiser, Papierfabr. **50**, 655 (1933).
[7] A. J. Stamm, Colloid Symposium Monograph **4**, 246 (1926); **5**, 361 (1927); **6**, 83 (1928).
[8] A. J. Stamm, J. Agr. Res. **38**, 23 (1929).
[9] A. J. Stamm, Physics **1**, 116 (1931).
[10] A. J. Stamm, J. Phys. Chem. **36**, 312 (1932).
[11] A. J. Stamm, Ind. Eng. Chem. **27**, 401 (1935).
[12] A. J. Stamm and W. K. Loughborough, J. Phys. Chem. **39**, 133 (1935).
[13] J. H. Sutherland, H. W. Johnston and O. Maass, Can. J. Research **10**, 36 (1934).
[14] A. C. Walker, J. Text. Inst. **24**, T145 (1933).

Further Studies on Mathematical Physics of Metabolizing Systems with Reference to Living Cells

N. RASHEVSKY, *University of Chicago*

(Received June 22, 1935)

In previous papers we studied the effects of forces, produced by metabolism, on the mechanical stability of the metabolizing system. In this paper various other effects of those forces are discussed. First of all it is shown that, whenever those forces are of such a nature as to make the system unstable and cause its eventual division, their effect is also that of increasing the size of the system. This reminds of the relation between rate of growth and division in living cells. Further the effects of those forces on molecules and colloidal particles, present in the system, but not directly participating in metabolism, are studied. It is shown that those forces produce a nonhomogeneous distribution of those molecules and particles, and thus alter the structure and the physical constants of the system. For single molecules the effect is negligible; but for colloidal particles of a size above 10^{-5} cm it may be very large and may produce a concentration of those particles at the surface of the system, altering thus the permeability of the latter. Those effects are present only as long as the system metabolizes. This may have a bearing on the sudden change of permeability of living cells after death. Since, under the influence of those forces the permeability of a system becomes a function of the intensity of the metabolizing processes, the fundamental equations describing such systems are much more complicated than those studied hitherto. One particularly interesting feature is that those equations now possess in general not one, but *several stable solutions*, so that the specification of all the parameters, which determine the external conditions, does not determine the configuration of the system in a unique way. As shown previously, such a situation leads to various hysteresis phenomena. One type of such a hysteresis, particularly interesting from the point of view of possible biological applications, is illustrated on a numerical example. It consists in an irreversible transition of the system from a state of slower growth and greater stability into a state of more rapid growth and lesser stability, under the influence of certain reversible changes in the environment of the system.

IN a series of previous papers,[1–4] we have shown that every metabolizing system is a seat of various forces, partly of osmotic, partly of atomic origin. Those forces are proportional to concentration gradients, produced by metabolism, and are therefore present only as long as the latter persists. We have investigated the effect of those forces on the mechanical stability of the system, and shown how they can cause a spontaneous division of the latter. In the present paper we shall study some other possible effects of those forces.

An important general effect of the forces produced by metabolism is their influence on the variation of the size of the system. As we have seen, substances diffusing inward produce osmotic forces, also directed inward, and tending to *compress* the system, while substances diffusing outward produce forces tending to *expand* the system. It is these expanding forces that produce under certain conditions, previously studied, a spontaneous division of the system. But these same expanding forces will tend also to increase the size of the system. Such an increase cannot go on indefinitely without some additional production of the substances, of which the system is composed. The expanding forces cannot therefore be the only factor, which would produce increase of size. But it is one of many possible other factors, which acts in the sense of increasing the size of the system. Other conditions being equal, the stronger the expanding forces, the more rapidly the system will increase in size. On the other hand, as we have seen,[4] the greater the expanding forces, the stronger will be the tendency of the system to divide spontaneously. In the particular case, studied previously,[4] of a complex metabolizing system, which decomposes glucose and partly oxidizes it, we have seen that the stronger the glycolysis, the less stable the system is mechanically, and the more readily it divides. But from what has just been said, the stronger the glycolysis, the more rapidly the system must also increase in size. This also agrees with observations on living cells, the only natural metabolizing systems so far known. Rapidly *growing* cells of embryonic tissues are characterized by a high rate of glycolysis. Still more

[1] N. Rashevsky, Physics **5**, 374 (1934).
[2] N. Rashevsky, Physics **6**, 35 (1935).
[3] N. Rashevsky, Physics **6**, 33 (1935).
[4] N. Rashevsky, Physics **6**, 117 (1935).

rapidly growing tumors have a still higher glycolytic coefficient. The exact mechanism of increase of size of metabolizing systems, depending on several factors, will be studied mathematically in a separate paper.

Another important effect of these forces is their influence on molecules and molecular aggregates, present in solution in the system, but neither diffusing in or out from the latter. Under those conditions their concentration will be uniform, unless this uniformity is disturbed by some force.

Let us first consider the "atomic forces" only. The same considerations as apply to the interaction between the molecules B of a nonuniformly distributed dissolved substance and a molecule A of the solvent,[1] hold also for the interaction between B and any *other* molecule C, dissolved in the system. In the most general case we should investigate also the mutual interaction of the molecules B. But this would mean that we cannot apply to B the laws of dilute solutions, and *for the present* we shall restrict ourselves only to those. However, even for a dilute solution, we do in general consider the interaction between the molecules of the solvent and the solute.[5]

Similarly, retaining the laws of dilute solutions for B, we may consider interactions between B and C.

The force, acting on a molecule C placed in a field of nonuniform concentrations of B, is given by Eq. (8) of a previous paper:[1]

$$g=\frac{4\pi KN}{M(n-1)(n-3)d^{n-4}}\operatorname{grad} c=a\operatorname{grad} c, \quad (1)$$

the notations being the same. If, instead of a single molecule, we consider a molecular complex, or colloidal particle, consisting of m molecules C, then the force will be

$$G=\frac{4\pi KNm}{M(n-1)(n-3)d^{n-4}}\operatorname{grad} c=ma\operatorname{grad} c. \quad (2)$$

With[6] $n=6$ and $d\sim 10^{-8}$ cm, we find $K\sim 10^{-53}$. This gives:

$$a\sim 10^{-15}. \quad (3)$$

Consider, for sake of definiteness, that the force g is directed from the center to the periphery of the system. The work necessary to bring a particle from the periphery to the center is equal to

$$\psi=\int_{r_0}^{0} G dr=a\int_{r_0}^{0}\operatorname{grad} c dr=ma(\bar{c}-c^0), \quad (4)$$

where $\bar{c}$ and c^0 denote the concentrations at the surface and at the center, respectively. We have:[1]

$$\bar{c}-c^0=gr_0/6D. \quad (5)$$

The ratio α of concentrations of the particles C at the surface and in the center, produced by the above forces, is given by Boltzmann's law:

$$\alpha=e^{-\psi/kT}. \quad (6)$$

In order that this ratio should be appreciably different from 1 we must have:

$$\psi\sim kT. \quad (7)$$

With values for q, r_0 and D used previously, we find: $\bar{c}-c^0\sim 10^{-5}$ g·cm^{-3}; combining this with (3) we find $\psi\sim m\times 10^{-20}$. Eq. (7) is therefore equivalent to

$$m\sim 10^{20}kT\sim 10^{6}. \quad (8)$$

(7) and (8) show, that the effect of the forces here discussed on single molecules is negligible, for then $\psi/kT\sim 10^{-6}$ and α is very near to unity. For a colloidal particle consisting of 10^6 molecules, that is having the size of $\sim 10^{-6}$ cm, α will be already of the order of 3. This means that there will be a very strong concentration of the particles C near the surface of the system. For particles of the order of magnitude of 10^{-5} cm $m\sim 10^{9}$ and $\alpha\sim e^{1000}$. This means that practically all particles C will be concentrated at the surface, forming a separate surface phase. In other words the forces due to concentration gradients will under certain conditions produce a radical change in the structure of the surface of the system. And this change of structure naturally must result in a change of permeability h. If the system stops metabolizing, or speaking biologically, dies, the forces disappear, and the particles C, concentrated at the surface, become distributed uniformly through the system. This is accompanied by a change in the permeability. It is known in biology that the *death* of a cell is

[5] M. Planck, *Treatise on Thermodynamics* (London, Longmans, Green and Co., 1927).
[6] A. Gyemant, *Grundzuge der Kolloidphysik* (Vieweg, Braunschweig, 1925).

accompanied by almost instantaneous changes in its permeability.

The osmotic forces, which are of the same order of magnitude as the other ones,[1] will produce similar effects. If V is the volume of the colloidal particle, then the total force acting on it is:

$$(RT\ V/M)\ \text{grad}\ c, \tag{9}$$

which is formally similar to (2). The calculation proceeds in the same way, and leads to similar results.

Of course the force may also be directed inwards and then produce a concentration of colloidal particles in the center of the system. This may result in the separation of a phase. In a complex system, consisting of many metabolizing substances and many different colloids, some particles will go one way, some the other. But in any case, the concentration gradients due to metabolism will produce a heterogeneity even in those components of the system which may not directly take a part in the metabolic processes.

In a previous paper,[3] we have shown that when the metabolized substances are ionized, the system will be the seat of electric charges, those charges disappearing when metabolism ceases. An excess of electric charges of any sign in the system has the effect of producing a "diffuse double-layer" at the surface.[6] For charges of the order of magnitude of those calculated before[3] the drop of potential φ across the double layer is of the order of magnitude of 10^{-2} volt.[6] The effect of such a double layer upon the permeability of the surface to ions is readily seen. A positive ion approaching the surface from the positive side will pass without other resistance than that due to the finite coefficient of diffusion. If the ion approaches the surface from the opposite side, in order that it should pass through, we must have $(1/2)mv^2 > 3\cdot 3\times 10^{-3}\ \varphi e$, m being the mass of the ion, v the normal component of its velocity, e the charge expressed in e.s.u. and φ being expressed in volts. In other words the permeability will be asymmetrical. The permeability h of a surface is defined by

$$n = h(c_1 - c_2), \tag{10}$$

where n denotes the number of molecules, passing per unit area per unit time, when c_1 and c_2 are numbers of molecules per unit volume on each side of the surface. We can therefore calculate the permeability of an electric double-layer for an ion in the "direction of smaller permeability," by putting $c_2 = 0$ and calculating the fraction $n/c_1 = h$ of the ions which can pass through the layer, that is the fraction for which $(1/2)mv^2 > 3\cdot 3\times 10^{-3}\ \varphi e$. This fraction is calculated in a similar way, like in the old theory of thermionic effect[7] with an electronic gas inside the metal, and a double layer at the surface.[7] In this way we find for the number of ions passing through in the "difficult direction" per cm^2 per second the expression

$$n_1' = c_1(k/2\pi m)^{\frac{1}{2}} T^{\frac{1}{2}} e^{-b/T} \tag{11}$$

with

$$b = 3\cdot 3\times 10^{-3}\varphi e/k. \tag{12}$$

The corresponding permeability is equal

$$h_1 = n_1/c_1. \tag{13}$$

The permeability of the other direction is obtained by putting $b = 0$. This permeability h_2 is also equal to the permeability in the same direction for ions of opposite charge. The ratio of the two permeabilities is equal to

$$h_1/h_2 = e^{-b/T}. \tag{14}$$

With $\varphi \sim 10^{-2}$ volt we find $b \sim 10^2$.

$$h_1/h_2 \sim 1/e. \tag{15}$$

A slight increase in φ causes a very large decrease of h_1/h_2. For $\varphi = 50$ millivolts, $h_1/h_2 = 0.04$.

This "elective permeability" for ions of one sign remains only as long as the electric charges remain, that is as long as the system metabolizes. As a rule living cells show an elective permeability for ions, which disappears after death. The present technique of permeability determination in single cells, which is largely qualitative, does not give any evidence for an "asymmetry" of the kind here discussed. But such an asymmetry for ions is not improbable in view of the fact that some biological membranes show an asymmetry even for neutral molecules.

As a general result we find that metabolic

[7] E. Bloch, *Thermionic Phenomena* (Methuen and Co., London, 1927).

processes affect by a purely physical mechanism the permeability of the system for the metabolized substances. Since this permeability in general may affect itself the metabolic processes, we arrive at a generalization of the previous treatments. We shall next have to consider h and D in our fundamental equations not as given constants, but as depending themselves on the distribution of concentrations which they effect.

The study of such general cases leads to a number of separate problems of various mathematical complexity. Mathematically each case will depend on the assumptions which we make about the nature of the colloidal substances, and about their influence on the permeability of the surface. These assumptions will determine how the permeability will vary with the concentration gradients, and since the latter in their turn depend on the rate of production or consumption of a substance, we shall thus study various possible laws of variation of h with the total rate Q of metabolism of a given substance. Amongst many possibilities a particularly interesting case is that when the $h-Q$ curve is S-shaped or inverted-S-shaped; that is for small Q, h is nearly constant, then in the neighborhood of a certain value Q^* it more or less suddenly increases or decreases, approaching, however, again an asymptotic value for very large Q. A curve of that type can be characterized by the initial value h, the final value h', the value Q^*, at which the curve has its inflection point, that is for which $|dh/dQ|$ is a maximum, and finally by the "half-width" ΔQ, which gives the distance along the Q-axis between the two points on the curve, for which $|dh/dQ|$ has half its maximum value. ΔQ is a measure of the steepness of the curve.

The detailed study of this case, which can be shown to be rather general, as well as of other possible cases, requires rather elaborate mathematical investigations, which must be reserved for separate papers. Here we shall confine ourselves to an illustration on an example of a particularly important characteristic of such cases.

Let us again consider a system in which glucose is partly glycolized, partly oxidized. However, instead of assuming, as we *approximately* did before, constant rates of reactions, we shall consider, in better agreement with actual facts, that the rates of reactions are proportional to the concentrations of the reacting substances.

For glucose we shall then have the differential equations and boundary conditions:

$$D_1\nabla^2 c_1 = ac_1; \quad \nabla^2 c_1' = 0;$$
$$h_1(c_1' - c_1) = D_1'(dc_1'/dr) = D_1(dc_1/dr) \quad \text{for } r = r_0, \tag{16}$$

the subscript $_1$ referring to glucose, the superscript $'$ referring to the external concentration. a is a constant characteristic of the reaction.

For lactic acid we have:

$$D_2\nabla^2 c_2 = ac_1 - fc_2c_3; \quad \nabla^2 c_2' = 0;$$
$$h_2(c_2' - c_2) = D_2'(dc_2'/dr) = D_2(dc_2/dr) \quad \text{for } r = r_0, \tag{17}$$

f being another constant, and the subscript $_2$ referring to lactic acid, and $_3$ to oxygen. Finally for oxygen we shall have:

$$D_3\nabla^2 c_3 = 1\cdot 07fc_2c_3; \quad \nabla^2 c_3 = 0;$$
$$h_3(c_3' - c_3) = D_3'(dc_3'/dr) = D_3(dc_3/dr) \quad \text{for } r = r_0. \tag{18}$$

We shall have a similar equation for CO_2. Because of the nonlinearity of the system (16), (17), (18) its general treatment presents great difficulties. We may, however, simplify considerably our problem and obtain a general semi-quantitative survey of the solution by using a device employed previously:[3] namely, we may consider with a sufficient approximation the case that all D's are, though finite, very large. Then the variation of concentrations inside and outside the system will be small as compared with the absolute values of the concentrations, and in calculating those values we may assume them to be uniform. We cannot assume the D's to be infinite, because then the gradients would vanish, and with them the forces which we are studying. But with finite, though sufficiently large D's, the gradients may be sufficient to produce the necessary forces, yet be small enough to justify the calculation of the concentrations on the assumption of their uniformity. A more rigorous justification of this procedure requires a detailed mathematical investigation of the general problem and shall be given elsewhere.

With this assumption the concentrations may

be calculated by the consideration that just as much substance enters (or leaves) the system as is consumed (or produced) in it.[3, 8] Our system of Eqs. (16)–(18) then becomes equivalent to

$$4\pi r_0^2 h_1(c_1'-c_1)=(4/3)\pi r_0^3 a c_1, \quad \text{(a)}$$

$$4\pi r_0^2 h_2(c_2-c_2')=(4/3)\pi r_0^3(ac_1-fc_2c_3), \quad \text{(b)} \quad (19)$$

$$4\pi r_0^2 h_3(c_3'-c_3)=1\cdot 07(4/3)\pi r_0^3 fc_2c_3, \quad \text{(c)}$$

where c_1', c_2' and c_3' are the *given* constant concentrations of glucose, lactic acid and oxygen in the external medium. To (19) must be added the equation for CO_2:

$$4\pi r_0^2 h_4(c_4-c_4')=1\cdot 47(4/3)\pi r_0^3 fc_2c_3. \quad (20)$$

The coefficients 1·07 in (19c) and 1·47 in (20) are determined from the stoichiometrical characteristics of the reactions considered.

The first Eq. (19) gives:

$$c_1=3h_1c_1'/(ar_0+3h_1). \quad (21)$$

Solving the third Eq. (19) with respect to c_3, and substituting into the second, we find after some rearrangements:

$$c_2=(3h_2/ar_0)c_2+[fh_3c_3'/(ah_3+0\cdot 36ar_0fc_2)]c_2 - 3h_2c_2'/ar_0. \quad (22)$$

If

$$0\cdot 36r_0fc_2 \ll h_3, \quad (23)$$

then (22) reduces to

$$c_1=[3h_2/ar_0+fc_3'/a]c_2-3h_2c_2'/ar_0. \quad (24)$$

Taking c_1 and c_2 as coordinates in a plane, let us plot the curves, represented by (21) and (24). If all h's are constant, then (21) represents a straight line, parallel to the c_2-axis, while (24) is another straight line, with a positive slope, intersecting the c_2-axis on the positive side. Hence the two lines will intersect in one point.

If (23) is not satisfied, then (22) represents a line, which is slightly convex upwards for small values of c_2, but which with increasing c_2 approaches asymptotically the straight line (24). There is again one and only one point of intersection between (21) and (22) for positive values of c_1 and c_2. The corresponding values of c_1 and c_2 represent the unique solution of our problem. Substituting those into the third equation (19) and into (20) we find also unique values for c_3 and c_4.

Things change, however, when the h's are not constant, but depend on the total rates of consumption of any of the substances, which rates determine the small but finite concentration gradients. Let us assume here, as an illustration only and for sake of simplicity, that the h's decrease with increasing Q_3, the total consumption of oxygen, according to an inverted-S-shaped curve discussed above, and are not influenced by either Q_1 or Q_2.

We have:

$$Q_3=4\pi r_0^2 h_3(c_3'-c_3). \quad (25)$$

Similar equations hold for Q_1 and Q_2.

Eq. (19) gives:

$$c_3=h_3c_3'/(0\cdot 36r_0fc_2+h_3), \quad (26)$$

which introduced into (25) expresses Q_3 as a function of h_3 and c_2:

$$Q_3=4\cdot 5r_0^3 fc_3'h_3c_2/(0\cdot 36r_0fc_2+h_3). \quad (27)$$

On the other hand we have the equations:

$$h_1=f_1(Q_3); \quad h_2=f_2(Q_3); \quad h_3=f_3(Q_3), \quad (28)$$

which express the permeabilities as a function of Q_3. Eliminating Q_3 from (27) and each of the Eqs. (28) we shall obtain three equations connecting h_1, h_2 and h_3 with c_2. From those we can express h_1, h_2 and h_3 as functions of c_2. If we introduce those expressions, which will depend on the assumption made about $f_1(Q_3)$, $f_2(Q_3)$ and $f_3(Q_3)$, into (21) and (24) we see that now those two equations do not represent any more straight lines, but more or less complicated curves, which may intersect *at more than one point.*

The analytical treatment of the problem would involve, even in the simplest case, rather elaborate calculations. A graphical solution is, however, very easily obtained. In Fig. 1, η represents the graph of Eq. (21), θ that of Eq. (24) for variable h's, with the following choice of constants:

[8] N. Rashevsky, Physics **1**, 143 (1931).

$$
\begin{aligned}
&r_0=3\times10^{-3}\,\text{cm};\quad a=0\cdot2;\quad f=40;\quad c_1'=10^{-3}\,\text{g}\cdot\text{cm}^{-3};\\
&\qquad c_2'=5\times10^{-4}\,\text{g}\cdot\text{cm}^{-3};\quad c_3'=10^{-3}\,\text{g}\cdot\text{cm}^{-2}.\\
&h_1=3\times10^{-4}\,\text{cm}\cdot\text{min.}^{-1};\quad h_1'=1\cdot6\times10^{-4}\,\text{cm}\cdot\text{min.}^{-1};\\
&\qquad Q_{31}^*=4\cdot4\times10^{-12}\,\text{g}\cdot\text{min.}^{-1};\quad \Delta Q_{31}=0\cdot8\times10^{-12}\,\text{g}\cdot\text{min.}^{-1}.\\
&h_2=3\cdot75\times10^{-4}\,\text{cm}\cdot\text{min.}^{-1};\quad h_2'=0\cdot9\times10^{-4}\,\text{cm}\cdot\text{min.}^{-1};\\
&\qquad Q_{32}^*=4\times10^{-12}\,\text{g}\cdot\text{min.}^{-1};\quad \Delta Q_{32}=1\cdot4\times10^{-12}\,\text{g}\cdot\text{min.}^{-1}.\\
&h_3=4\times10^{-4}\,\text{cm}\cdot\text{min.}^{-1};\quad h_3'=2\times10^{-4}\,\text{cm}\cdot\text{min.}^{-1};\\
&\qquad Q_{33}^*=4\times10^{-12}\,\text{g}\cdot\text{min.}^{-1};\quad \Delta Q_{33}=1\cdot4\times10^{-12}\,\text{g}\cdot\text{min.}^{-1}.
\end{aligned}
\tag{29}
$$

The constants are chosen so as to have biologically plausible values. Q_{31}^*, Q_{32}^*, Q_{33}^* are the values of Q_3^* for the inflection point of h_1, h_2 and h_3 correspondingly. ΔQ_{31}, ΔQ_{32} and ΔQ_{33} are the corresponding half-widths. We see that the two curves intersect at three points A_1, A_2 and A_3. For all points of the curve η Eq. (19a) is satisfied. All points in the c_1c_2-plane, which lie above η, correspond to such values of c_1 and c_2 for which the left-hand side of (19a) is smaller than the right-hand side. This means that for any such points there is less glucose penetrating into system than there is consumed. Hence $dc_1/dt<0$ and c_1 will decrease until a point on the η-curve is reached. For all points below η the reverse holds true. c_1 increases until η is reached. For all points above θ the left-hand side of (19b) is smaller than the right-hand side, hence $dc_2/dt>0$ and c_2 increases. The reverse holds true for all points below the curve θ. Those considerations show that the points A_1 and A_3 represent *stable* solutions of (19), whereas A_2 is unstable. A slight displacement in the c_1c_2-plane from the point A_2 will result in such variations of c_1 and c_2 that either A_1 or A_3 will be reached.

We find from Fig. 1 and Eq. (25) and (29) that for A_1:

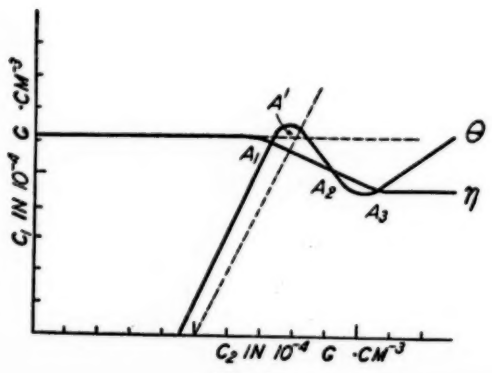

FIG. 1.

$$
\begin{aligned}
&Q_1=13\times10^{-12}\,\text{g}\cdot\text{min.}^{-1};\\
&Q_2=9\cdot4\times10^{-12}\,\text{g}\cdot\text{min.}^{-1};\\
&Q_3=3\cdot7\times10^{-12}\,\text{g}\cdot\text{min.}^{-1}.\quad \beta=0\cdot9
\end{aligned}
$$

for A_3: (30)

$$
\begin{aligned}
&Q_1=10\cdot3\times10^{-12}\,\text{g}\cdot\text{min.}^{-1};\\
&Q_2=5\cdot6\times10^{-12}\,\text{g}\cdot\text{min.}^{-1};\\
&Q_3=5\cdot2\times10^{-12}\,\text{g}\cdot\text{min.}^{-1}\quad \beta=0\cdot4
\end{aligned}
$$

where β denotes the glycolytic coefficient.[4] We see that in A_1 the relative production of lactic acid is higher and β much larger.

We thus see that whereas in the previously studied cases of constant h the physico-chemical configuration of the system was determined in a unique way by the parameters which characterize the external medium (such as c_1', c_2' and c_3'), now we find that the system possesses in general several configurations of equilibria. We have already made previously[9] a study of the general properties of such systems, and seen that they are characterized by various hysteresis phenomena in which a reversible change of the external conditions produces an irreversible change in the system. Let, for instance, the system have the configuration A_3. If we reduce sufficiently c_3' (the supply of oxygen), then because of a decreased Q_3 all h's will increase to the corresponding maximum values, η and θ will become practically straight lines, intersecting at the point A'. (Fig. 1, broken lines.) If we again restore the original value (10^{-3} $\text{g}\cdot\text{cm}^{-3}$) for c_3', we shall find that the system will pass into configuration A_1, and not into the original A_3, because A' lies in a region of the c_1c_2-plane for which $dc_1/dt<0$ and $dc_2/dt<0$. The same thing will happen if, with the system originally in A_3, we temporarily reduce or make zero f. In configuration A_3 the system is char-

[9] N. Rashevsky, Zeits. f. Physik **53**, 102 (1929); **59**, 562 (1930); **61**, 511 (1930).

acterized by a lower permeability and a lower glycolytic coefficient. In A_1 both are increased. The situation represents a remarkable analogy to the fact discovered by O. Warburg,[10] that temporary asphyxiation of living cells may cause them to pass into a condition of higher glycolytic coefficient, and higher permeability, characteristic of tumor cells, and that this condition remains even after normal oxygen supply is reestablished.

The above example is used only as an illustration. Similar cases of hysteresis are obtained also with $dh/dQ_3>0$. Of course such "multiple equilibria" do not *always* occur in cases of variable h's, but their occurrence is rather general. We may consider also the more general case that the glycolysis is partly reversible, so that part of the lactic acid is transformed back into glucose. This complicates somewhat the calculations, but leaves the general result unchanged.

In the more general cases, when we consider also the role of the diffusion coefficients, still more complex conditions, with more than two stable equilibria, may occur. All this will be made a matter of future studies.

[10] O. Warburg, *The Metabolism of Tumors* (Constable and Co. London, 1930).

Notice to Contributors

Manuscripts

Send manuscripts to John T. Tate, University of Minnesota, Minneapolis, Minnesota.

Papers must be in English, typewritten double spaced with wide margins.

Abstracts

An abstract must accompany each article. It should be adequate as an *index* and as a *summary*. As an index it should give all subjects, major and minor, concerning which new information is presented. As a summary it should give the conclusions of the article and all numerical results of general interest.

References

References should appear as footnotes, numbered consecutively, and arranged thus:

A. B. Smith, Phys. Rev. **41**, 852 (1932).

Captions and Legends

Legends for figures must accompany manuscript. Each table should have a caption. These in all cases should be complete in themselves so as to make the data intelligible to the reader without reference to the text.

Mathematical Expressions

Make all expressions clear to the typesetter. Identify in the margin of the manuscript Greek letters and unusual symbols.

Use fractional exponents instead of root signs.

Avoid complicated exponents and subscripts. Should it be necessary to repeat a complicated expression a number of times it should be represented by some convenient symbol.

The solidus (/) should be used wherever possible for fractions.

Illustrations

Plan figures for approximately one-half reduction. Wherever possible arrange figures so that after reduction they will not be wider than three inches. Lettering must be large enough to be readable after reduction.

Line drawings must be made with India ink on white paper or tracing cloth. Coordinate paper is not desirable, but if used must be blue-lined and all coordinates to be reproduced drawn with India ink.

Drawings which cannot be used will be returned to the author or redrawn at his expense.

Photographs should show clear black and white contrasts.

Avoid round and oval photographs.

Publication Charge

A portion of the cost of publishing the results of research must be regarded as an integral part of the cost of the research. In keeping with the policy which is effective for the Institute's publications a bill for $3.00 per page will be sent to the authors of papers appearing in this journal. It is intended that the authors shall present these bills for payment to the institutions which have supported their researches. If the institution is unable to make payment the bills are to be returned marked "No Funds Available."

Reprints

As a partial return for the publication charge one hundred reprints without covers will be furnished free. Additional reprints may be obtained at a regular schedule of prices.

Alterations

Take great care that each manuscript is typographically accurate. A limited number of alterations in proof are unavoidable, but the cost of making extensive alterations after the article has been set in type will be charged to the author.

Proof and all correspondence concerning papers in the process of publication should be addressed to the Editorial Secretary, American Institute of Physics, 11 East 38th Street, New York, N. Y.

THE AMERICAN PHYSICAL SOCIETY

R. W. WOOD, *President*
The Johns Hopkins University
Baltimore, Maryland

F. K. RICHTMYER, *Vice President*
Cornell University
Ithaca, New York

W. L. SEVERINGHAUS, *Secretary*
Columbia University
New York, New York

G. B. PEGRAM, *Treasurer*
Columbia University
New York, New York

JOHN T. TATE, *Editor*
University of Minnesota
Minneapolis, Minnesota

L. B. LOEB, *Local Secretary for the Pacific Coast*
University of California
Berkeley, California

THE object of the American Physical Society is the advancement and diffusion of the knowledge of physics. It sponsors *The Physical Review*, *Physics* and the *Reviews of Modern Physics*. Upon the recommendation of two or more members, any person engaged in work in the field of physics or actively interested in physics may become a member; receive one of the journals; receive also *Science Abstracts* A, and the Bulletin of all meetings; and attend and participate in the seven annual meetings.

Annual dues: $10. Fellows, $14.

For further information address the Secretary as above.

THE SOCIETY OF RHEOLOGY

S. E. SHEPPARD, *President*
Eastman Kodak Company
Rochester, New York

EUGENE C. BINGHAM, *Editor*
Lafayette College
Easton, Pennsylvania

A. STUART HUNTER, *Secretary & Treasurer*
Du Pont Rayon Company
Buffalo, New York

THE Society of Rheology was formed in 1929 to advance the science of the deformation and flow of matter. It cooperates with the American Physical Society in editing *Physics* of which four issues per year are devoted to *Rheology*. All persons interested are invited to become members and participate in the proceedings at the annual meetings. Members receive without other charge than their dues all issues of *Physics* and the notices of the Society.

Annual dues: $6.

For further information address the Secretary as above.